

Otoprotection of Metformin in Radiation-Induced Sensorineural Hearing Loss

Mario Mujica-Mota, MD

Department of Otolaryngology
McGill University, Montreal

December 2012

A thesis submitted to McGill University in partial fulfillment of the requirements for
the degree of Master of Science

Copyright © 2012 Mario Mujica-Mota

TABLE OF CONTENTS

List of Abbreviations	iv
Abstract.....	v
Résumé	vi
Acknowledgements	viii
 PART ONE: Introduction	 1
<i>Chapter 1.1. Introduction</i>	1
<i>Chapter 1.2. Thesis rationale, objectives and organization</i>	3
 PART TWO: Background & Literature review	 4
<i>Chapter 2.1. Basic anatomy and physiology of hearing</i>	4
The external and middle ear	4
The cochlea	5
Cochlear mechanics and nerve transmission.....	7
<i>Chapter 2.2. Radiobiology of radiation and radiotherapy</i>	10
Principles of radiobiology	10
Fractionation & its rationale.....	11
Dose and functional damage	12
<i>Chapter 2.3. Radiation-induced damage to the ear.</i>	14
Radiotherapy & the ear	14
External ear	15
Middle ear	15
Inner ear	15
<i>Chapter 2.4. Methods for audiological monitoring of radiation-induced sensorineural hearing loss</i>	16
Behavioral pure tone audiometry	16
Distortion Product Otoacoustic Emissions.....	17
The Auditory Brainstem Response	18
<i>Chapter 2.5. Characteristics of radiation-induced sensorineural hearing loss. A systematic review.</i>	20
Introduction	20
Methods.....	20
Results	21
Discussion	25
Conclusions	31
<i>Chapter 2.6. Mechanism of radiation-induced sensorineural hearing loss.</i>	32
Molecular mechanisms of radiation-induced cochlear damage	32
Evidence from animal models of radiation-induced cochlear damage	34

<i>Chapter 2.7. Radioprotection and radiation-induced cochlear damage.</i>	36
Radioprotection	36
Models of radiation-induced cochlear damage & radioprotection	37
<i>Chapter 2.8. Metformin.</i>	39
Characteristics of Metformin	39
Metformin as a reactive oxygen species regulator	40
Metformin as an anticancer agent.	41
Metformin and its interference with radiotherapy	42
PART THREE: Experimental studies	43
<i>Chapter 3.1 Introduction & overall experimental plan.</i>	43
<i>Chapter 3.2. In vitro estimation of the cytotoxic and radioprotective effects of Metformin.</i>	44
Introduction	44
Objective	44
Methods	44
Results	46
Discussion	48
Conclusion	48
<i>Chapter 3.3. Methodology for controlled radiation of the guinea pig cochlea</i>	49
Introduction	49
Objectives	50
Methods	50
Results	55
Discussion	57
Conclusion	61
<i>Chapter 3.3. In vivo evaluation of radio-protective effects of Metformin in the guinea pig cochlea.</i>	62
Introduction	62
Objective	62
Methods	62
Results	66
Discussion	68
Conclusion	70
PART FOUR: Overall Conclusion	71
<i>Chapter 4.1. Conclusion</i>	71
References	72

List of Abbreviations

2D- two dimensional; 3D- three dimensional
ABR- Auditory Brainstem Response
AMPk- Adenosine monophosphate protein kinase
CM- cochlear microphonics
dB- decibels; dB HL – decibels hearing level
DPOAE- Distortion Products Otoacoustic Emissions
DSB- double-strand break
EAC- external auditory canal
EORTC- European Organization for Treatment of Cancer
FR- Fractionated Radiotherapy
GP-Guinea pig
Gy- Gray
H₂O₂- Hydrogen peroxide
OH- hydroxyl radical
H&N- Head and Neck
Hz- Hertz; kHz- kiloHertz
IHC- Inner hair cells
IMRT- Intensity modulated radiotherapy
kV- kilovolt
LENT/SOMA- Late Effects Normal Tissue-Subjective, Objective Management and Analytic scale
LSO- lateral superior olivary complex
mA- milliamperes
mm- millimeter
MSO- medial superior olivary nucleus
MtDNA- mitochondrial DNA
mV- millivolt
MV- megavolt
NPC- Nasopharyngeal Carcinoma
OHC- Outer hair cells
RISNHL- Radiation-induced sensorineural hearing loss.
ROS- Reactive Oxygen Species
RT- Radiotherapy
RTOG – Radiation Therapy Oncology Group
SNHL- Sensorineural Hearing Loss
SRS- stereotactic radiosurgery
TLD- Thermoluminescent dosimeter

Abstract

Introduction: Radiotherapy can cause permanent hearing loss when the ears are included in the radiation field. To date, no treatment is available to prevent this outcome. The effects of radiation are caused by free radical formation, leading to apoptosis of the cells in the organ of Corti. Metformin has demonstrated anticancer and anti-aging properties through the regulation of reactive oxygen species production after cellular stresses.

Objectives: To determine the safety and radio-protective properties of Metformin against radiation-induced cochlear damage *in vivo* and *in vitro*.

Materials and Methods: For the *in vitro* study, cultured auditory hair cells (HEI-OC1) were exposed to different concentrations of Metformin to determine its safety. Next, cells were incubated with these concentrations and subjected to radiation. Cell viability after experiments was determined with the 3-(4, 5-dimethylthiazol-2-yl)-5-(3-carboxymethoxyphenyl)-2-(4-sulfophenyl)-2H-tetrazolium (MTS) assay. For the *in-vivo* study, 15 guinea pigs were divided in two groups: drinking tap water (n=7) and drinking water containing Metformin (n=8) at a dose of 100 mg/kg/day. The ears of the animals were unilaterally irradiated for 20 days (total dose 71 Gy) and subsequently divided in four groups: Control (n=7), Irradiated (n=7), Metformin (n=8), Experimental (n=8). Distortion Products Otoacoustic Emissions (DPOAE) and Auditory Brainstem Responses (ABR) were assessed before, one week and six weeks after completion of radiotherapy.

Results: Metformin was not ototoxic or radio-protective in cultured auditory hair cells. DPOAE measurements did not show hearing loss or differences between the four groups at the different time points evaluated. After 6 weeks, ABR demonstrated progressive hearing loss. Experimental ears had less hearing loss than radiated ones; however, differences were not statistically significant.

Conclusion: Metformin is not ototoxic *in vitro* or *in vivo*. Metformin was not protective against radiation induced cell death *in vitro*.

Résumé

Introduction: La radiothérapie peut provoquer une perte auditive permanente quand l'oreille est incluse dans la zone de radiation. Il n'y existe aucun traitement préventif pour cet effet néfaste. La radiation provoque la formation des radicales libres entraînant la mort de cellules dans l'organe de Corti. La Metformine, un médicament vastement utilisé dans le traitement du diabète a montré des propriétés anticancéreuses et antiviellissement par la régulation de la production d'espèces réactives de l'oxygène après le stress cellulaire.

Objectifs: Déterminer l'ototoxicité et les propriétés radio-protectives de la Metformine contre l'atteinte cochléaire provoqué par radiation *in vivo* et *in vitro*.

Matériaux et méthodes: Les cellules auditives cultivées (HEI-OC1) ont été exposées à différentes concentrations de Metformine pour déterminer le potentiel d'ototoxicité de ce dernier. En plus, les cellules ont été incubées avec diverses concentrations et par la suite, exposées à la radiation. La survie cellulaire a été déterminée par la méthode MTS.

Quinze cochon d'Inde ont été divisés en deux groupes: buvant de l'eau potable (n=7) et buvant de l'eau contenant la Metformine (n=8) avec une dose de 100 mg /kg/jour. Les oreilles des animaux ont été irradiées unilatéralement pendant 20 jours (dose totale 71 Gy) et par conséquent ont été divisées en quatre groupes: Control (n=7), Irradiées (n=7), Metformine (n=8), Expérimentales (n=8). Les Produits de Distorsion des Émissions Otoacoustiques (PDEO) et les Réponses Auditives du Tronc Cérébral (RATC) ont été six semaines après la radiothérapie.

Résultats: La Metformine n'est pas été ototoxique ou radio-protective des cellules auditives cultivées. Les PDEO test n'ont pas montré de perte auditive ou de différences entre les quatre groupes aux différents temps évaluées. Après six semaines. Les oreilles expérimentales ont eu moins de perte auditive comparées aux oreilles irradiées, néanmoins les différences n'ont pas été significatives.

Conclusion: La Metformine n'est pas ototoxique *in vitro* ou *in vivo*. La Metformine n'a pas été otoprotective *in vitro* ou contre la perte auditive causée par radiation après un suivi de six semaines après la fin de la radiothérapie.

To my parents and brothers,
who taught me the richness of learning.

Acknowledgements

I would like to express my deep gratitude to my supervisor Dr. Sam J. Daniel for his guidance, support and patience through the completion of this work. His encouragement and his personal and professional example provided an excellent basis for my studies. Also I would like to thank Dr. Bernard Segal for his mentorship in the preparation of this thesis.

I would like to address my sincere thanks to Dr. George Shenouda, the chairman of my committee; and the rest of the members Dr. Shirley Lehnert and Dr. Slobodan Devic for their constructive comments and for their supply with some of the tools I needed to develop this work. Having such enlightened minds as supervisors was an honor.

I would also like to thank my colleagues of the McGill Auditory Sciences Lab who were always eager to help. First, Mr. Dan Citra who helped me with some of the technical difficulties I faced during the animal experiments. I also thank Dr. Pezhman Salehi, Dr. Sofia Waissbluth, Dr. Victoria Akinpelu, Aren Bezdjian and Farid Ibrahim for their support during the process of this work. I also would like to thank to the staff of the Room B-240 and to the Montreal Children's Hospital library staff and workshop for their help.

Last but not least, I wish to thank to my parents for their infinite love and support and to my brothers Miguel and Tania who always helped and advised me. I would like to extend my deep gratitude to my family in Canada, the Gasbarrino family, in particular to Karina who has been always a source of motivation.

This work was supported from Grants from

The Department of Otolaryngology Head and Neck Surgery –McGill University

The National Council of Science and Technology-Mexico and

The Max Stern Recruitment Fellowship McGill University

Contribution of co-authors of specific chapters:

Chapter 6: Sofia Waissbluth approved the final version of the chapter.

Chapter 11: Slobodan Devic extracted data and approved the final version of the chapter.

Chapter 10: Pezhman Salehi extracted the data.

PART ONE: Introduction

Chapter 1.1. Introduction

The advance in knowledge and technology has led to an improvement in cancer treatment with a subsequent increase of cancer survivors. As a consequence, the importance of late effects of oncology treatment has been recently coming into closer scrutiny. In Canada, over 4300 patients will be diagnosed with a Head and Neck cancer every year ⁽¹⁾. Radiotherapy (RT) is a vital component in treatment protocols for most of these patients. While some radiation-induced complications are transient, sensorineural hearing loss (SNHL) is a late and permanent complication that is seen in many cases ⁽²⁾. Radiation-induced sensorineural loss (RISNHL) is present particularly in patients with parotid and nasopharyngeal carcinoma (NPC) whose inner ear is included within the radiation field⁽³⁾. In these patients, the majority of the dose delivered to the primary tumor also reaches the nearest cochlea (60-94% for parotid⁽⁴⁾ and up to 102% for NPC ⁽⁵⁾). Hence the risk of developing SNHL.

Radiation-induced sensorineural hearing loss is believed to result from damage to the auditory hair cells of the cochlea by means of apoptosis ⁽⁶⁾. However, it is believed that a triggering mechanism of radiation-induced cell death is the generation of reactive oxygen species (ROS) ^(7, 8). This is concordant with other etiologies of sensorineural hearing loss such as aging, noise exposure and drug toxicity where ROS production is an initial mechanism that leads to a final apoptotic pathway ⁽⁶⁾.

Experimental attempts to prevent radiation-induced cochlear damage in preclinical studies have been performed. However, in the current clinical practice there is no approved agent for the prevention of RISNHL. Therefore, an ideal preventative agent providing protection to the ear from radiation without intervening with cancer therapy is yet to be discovered.

Recent epidemiological, preclinical and clinical evidence supports the notion that Metformin has antineoplastic benefits in different types of cancer ^(9, 10). Contrasting

the effect in cancer, normal cells can undergo the metabolic adaptation promoted by Metformin without any damage⁽¹¹⁾. This is shown by the protective role of Metformin on normal cells subjected to stressors known to cause damage due to generation of ROS^(12, 13). For example, it has been demonstrated that Metformin prevented gentamicin ototoxicity *in vitro* by limiting the production of ROS production⁽¹⁴⁾. These results give insight into the potential benefits of Metformin.

Given the potential benefit of Metformin in cancer treatment and the evidence previously outlined, this thesis will evaluate the radioprotective properties of Metformin in a cochlear cell line and in a scheme of fractionated radiotherapy in a guinea pig animal model.

Chapter 1.2. Thesis rationale, objectives and organization

In view of the background previously outlined, this study aimed to test the effect of Metformin on radiation-induced cochlear damage. To do this, both *in vitro* and *in vivo* experiments were planned. Experiments were performed in a cochlear hair cell line and in a guinea pig animal model of radiation induced hearing loss.

The overall objective of thesis will be to assess the ototoxicity of Metformin and to investigate its protective effects against radiation-induced cochlear damage *in vitro* and *in vivo*.

The working hypothesis of this thesis is that Metformin can prevent or reduce the damage caused by radiation in auditory hair cell lines and in a guinea pig animal model of fractionated radiotherapy.

The thesis will be divided in four more parts starting with a literature review in Part two including anatomical concepts of the peripheral auditory pathway and the radiobiology of radiation and radiotherapy (Chapter 2.1 and 2.2); the damage caused by radiotherapy to the ear structures and the main methods for their audiological monitoring as well a systematic review of the characteristics of RISNHL (Chapters 2.3 to 2.5) and finally the mechanisms of RISNHL, the concept of radioprotection and the characteristics of Metformin(Chapter 2.6 to 2.8). The experiments performed and their results will be discussed in Part three. Part four will conclude this thesis.

PART TWO: Background & Literature review

Chapter 2.1. Basic anatomy and physiology of hearing

The hearing tests performed in the experiments of this thesis will assess the integrity of the auditory pathway, therefore basic concepts of anatomy and physiology will be presented in this chapter. The auditory system is delimited by the pinna and the primary auditory cortex in the left temporal lobe ⁽¹⁵⁾. An overview of the relevant structures for this study will be reviewed.

The external and middle ear

The peripheral auditory system is divided in three main parts which are delimited by anatomical structures (overviewed by Salvi⁽¹⁵⁾). The pinna and the external ear canal serve to direct the waves of sound in the environment towards the tympanic membrane, which is the main division between the external and middle ear. The tympanic membrane serves as a drum that vibrates after the waves enter in contact with it. This energy is transmitted through the chain formed by the three middle ear ossicles (malleus, incus and stapes), which together amplify the energy obtained at the tympanic membrane in the footplate of the stapes⁽¹⁵⁾. This last structure is attached to the oval window membrane at the base of the cochlea in such a way that it moves with every vibration (Figure 1).

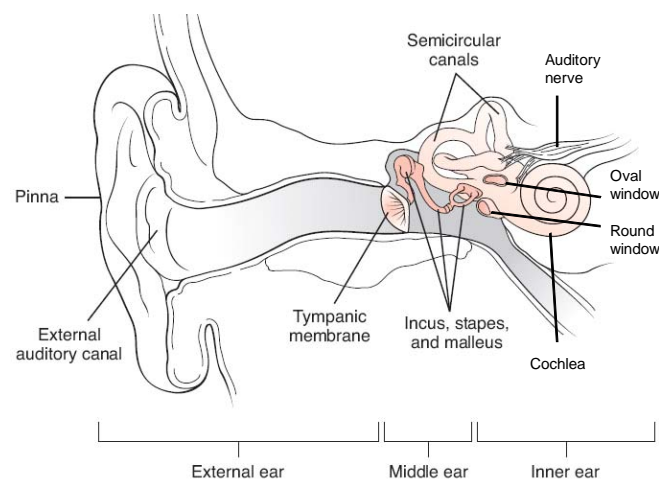


Figure 1. The peripheral auditory system. Adapted from Ream T.D. ⁽¹⁶⁾ with permission.

The cochlea

As part of the inner ear and enclosed in the temporal bone, the cochlea is the main hearing organ, consisting of three fluid-filled compartments coiled in two and a half turns⁽¹⁵⁾. Inside the scala media, the organ of Corti rests above the basilar membrane in a compartment also bounded by the Reissner's membrane and the lateral wall of the cochlea (Figure 2). The scala vestibuli has in its basal end the oval window, which is in contact with the stapes footplate⁽¹⁵⁾ and is the place where the sound-induced vibrations are transmitted to the cochlear fluids in the inner ear.

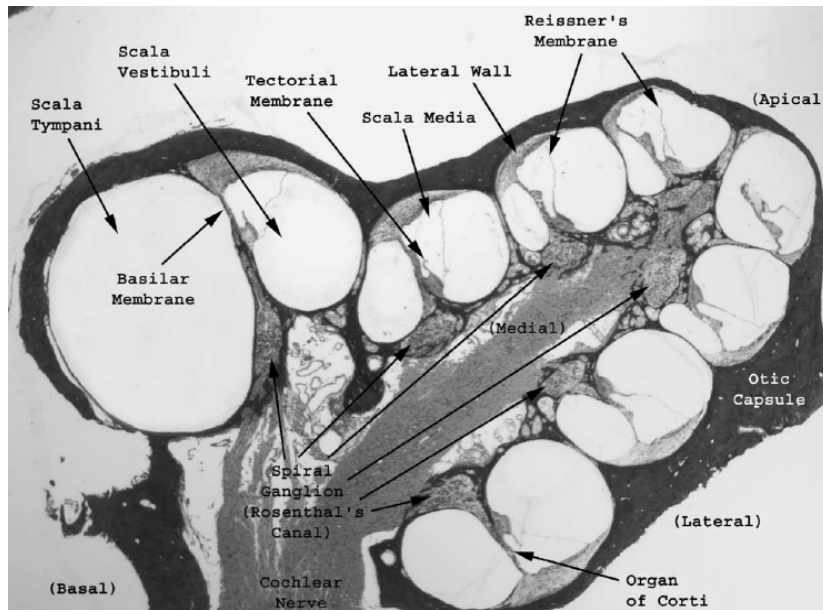


Figure 2. The cochlea in a mid modiolar section. From Raphael, Y.⁽¹⁷⁾ with permission.

As detailed by Salvi, the auditory hair cells located in the organ of Corti act as transducers through their stereocilia, converting the sound-induced vibrations into electrical activity promoting depolarization of the spiral ganglion neurons⁽¹⁵⁾. These hair cells are classified into inner hair cells (IHC) and outer hair cells (OHC)⁽¹⁸⁾. Furthermore, the tectorial membrane, a thin membrane attached over the stereocilia of the hair cells, follows the movement of these after the sound-induced vibrations reach the cochlea⁽¹⁵⁾. This arrangement allows the proper transmission of mechanical energy to hair cells with every sound-induced transmitted vibration into the cochlear fluids (Figure 3).

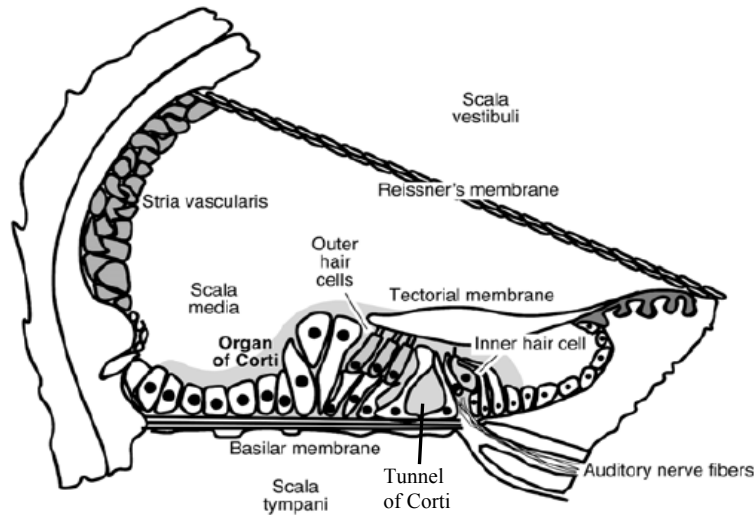


Figure 3. Cochlear section in the basal turn. From Van De Water T.⁽¹⁹⁾ with permission.

Endolymph, perilymph and auditory hair cells

The integrity of the OHC along with the homeostasis of the ionic composition in the cochlear fluids serve as a physiological basis of the Otoacoustic emissions, a test which will be described later. The perilymph ionic composition resembles the extracellular fluid with high content of sodium (150 millimol/L) and low potassium (3 millimol/L) while the endolymph contains ionic concentration resembling the intracellular fluid⁽²⁰⁾. The maintenance of these concentrations depends on adenosine triphosphate (ATP) dependent pumps that are located within the stria vascularis⁽¹⁵⁾. This difference in ionic concentration sets the membrane potential for proper hair cell depolarization.

The stereocilia of the hair cells (Figure 4) are formed from groups of actin filaments that are attached with side links near their base⁽¹⁹⁾. These links allow all the stereocilia to move in the same direction when the sound-induced vibrations reach the cochlea. Having this disposition, the deflection of the stereocilia causes the opening of potassium channels in the hair cell resulting in depolarization⁽²¹⁾ and transmission to the spiral ganglion neurons.

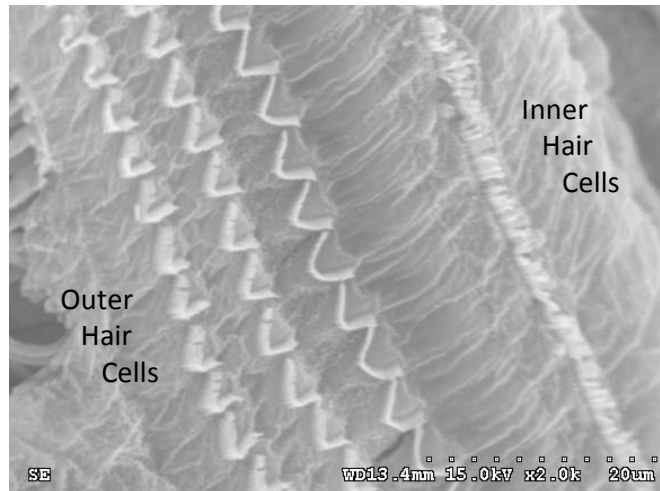


Figure 4. OHC and IHC stereocilia configuration. McGill Auditory Sciences Laboratory.

Cochlear mechanics and nerve transmission

As reviewed by Gillespie, the cochlea acts as a selective transducer depending on the intensity and frequency of the stimulus presented⁽¹⁹⁾. Due to mass (gradually increase) and stiffness variation (gradually decrease) from base to apex, the basilar membrane vibrates at specific frequencies along the cochlea⁽¹⁹⁾. Due to these characteristics, high frequency sounds produce a wave that peaks in the base and low frequency sounds do it in the apex⁽¹⁵⁾, making the basilar membrane acting as a piano keyboard (Figure 5).

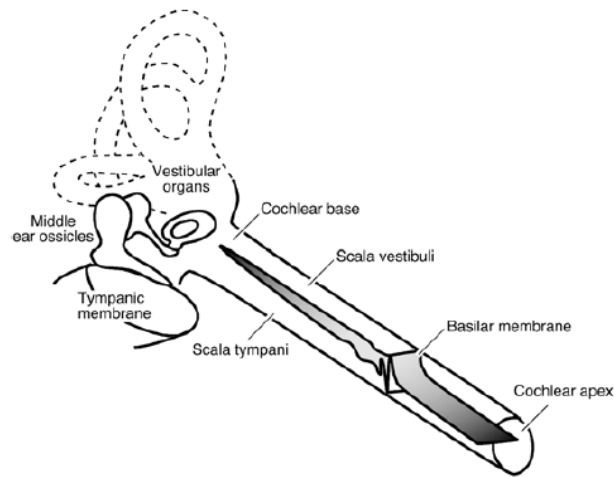


Figure 5. Travelling wave in the basilar membrane. From Van De Water T.⁽¹⁹⁾ with permission.

The axons of the spiral ganglion neurons form the auditory nerve, making synapses with cochlear nucleus at the level of the brainstem⁽¹⁵⁾, where the central auditory pathway begins. The next paragraphs will discuss the central pathways relays in ascendant order.

The central auditory pathway

The main relays of the pathway serve as an anatomical basis for the Auditory Brainstem Response (ABR), which will be used in the experimental part of this thesis. The central auditory pathway is demarcated by the cochlear nucleus and the auditory cortex in the temporal lobe⁽²²⁾ and is responsible for the integration of sound stimuli.

Evidence showed that unilateral damage at the cochlear nuclei can cause hearing disorders similar to auditory nerve dysfunction⁽²³⁾, demonstrating that cochlear nucleus has only ipsilateral input. The next relay is the contralateral superior olivary complex (SOC) consisting of three main groups of nuclei⁽²²⁾: the lateral superior olivary nuclei (LSO), the medial superior olivary nucleus (MSO), the nucleus of the trapezoid body (MNTB). The lateral lemniscus connecting the SOC with the inferior colliculus contains fibers from bilateral origins of the cochlear nucleus and SOC⁽²⁴⁾. As illustrated in Figure 6, the SOC and the inferior colliculus have bilateral input, which implies that they play a major role in interpretation of binaural sound stimuli.

At the level of the midbrain, the inferior colliculus, contains neurons with sharply defined frequency sensitivity⁽²⁵⁾ which suggests that is a relay where the stimuli are markedly differentiated in order to be properly integrated before passing to higher levels of the pathway. Finally, the medial geniculate body in the thalamus is the last relay before reaching the auditory cortex⁽²²⁾.

As described in detail by the work of Musiek⁽²⁶⁾, and similar to the arrangement in the cochlea, the neurons of the central auditory pathways always maintain a tonotopic arrangement⁽²⁷⁾, supporting the idea of a highly organized system involved in the integration of sound in the central nervous system.

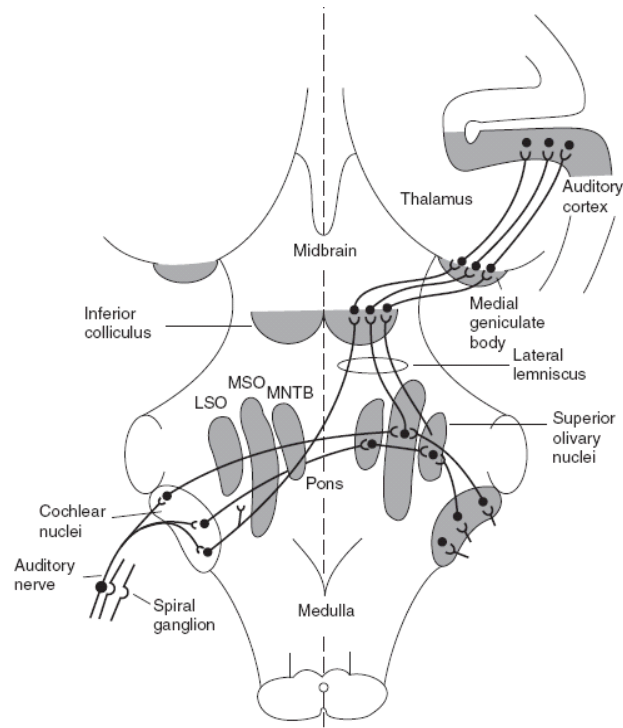


Figure 6. Schematic representation of the central afferent auditory pathway. From Middlebrooks JC, Squire, L. ⁽²⁸⁾ with permission.

Furthermore, the central pathway is connected to the reticular system, which enables to integrate the information received from sound stimuli in the cortex and to elicit a response⁽²²⁾. The reticular system has two main systems: the ascending reticular activating system and the motor activating system⁽²⁹⁾. With this interconnection, when the sounds represent danger to the subject, the cortex is activated and able to promote awareness and activation of the motor system to react.

While the auditory hair cells in the cochlea are the main signal transducers for sound stimuli, the central auditory pathway integrates the information to elicit a response to sounds. Furthermore, the auditory pathway has a high level of organization in order to accomplish these functions.

Chapter 2.2. Radiobiology of radiation and radiotherapy

In this chapter, basic concepts of radiobiology that will help understanding of the effects of radiation in the ear will be discussed. Despite that many of these concepts are oriented towards cancer cells, this chapter will intend to present the concepts in terms of adverse effects in normal tissue.

Principles of radiobiology

As reviewed by Hall and Cox (p. 4)⁽³⁰⁾, radiotherapy produces ionizations when it passes through molecules or tissues. Ionization occurs when the radiation has enough energy to eject electrons from the molecules present in the irradiated tissue or material⁽³⁰⁾.

X-ray radiotherapy is obtained from linear accelerators that increase the energy levels of electrons and then stop them abruptly in a target resulting in a focused beam of photons⁽³¹⁾. Their deep penetrating capacity is due to their high energy levels in the range of 110 kV - 18 MV⁽³¹⁾. However, an important factor to consider is the attenuation that these energies present depending on the density of the tissue irradiated⁽³²⁾. This concept is the basis of tissue depth-dependent dose absorption used in therapeutic radiation.

As outlined by Sharma et al.⁽³¹⁾, ionizing radiation exerts its effect by the “Compton effect” where the original ejected electrons in the target tissue also interact with surrounding tissue propagating the ionization until the energy dissipates. The ionization can result in direct and indirect damage to the deoxyribonucleic acid (DNA)⁽³¹⁾. While the former occurs within the DNA, the latter refers to the subsequent free radical formation that causes indirect damage to surrounding molecules⁽³¹⁾. Furthermore, it is believed that the latter mechanism is more important, supported by studies demonstrating the formation of ROS before DNA damage in cells subjected to radiation⁽³³⁾, suggesting the notion that free radicals are initiators of lethal cell damage.

In addition, it has been accepted that the most relevant chromosomal lesions after irradiation are double strand DNA breaks (DSB)⁽³⁰⁾. Since single strand DNA breaks can be relatively easily repaired with the opposite DNA strand, DSB can cause loss of cellular reproducibility, apoptosis, mutation or carcinogenesis⁽³⁴⁾. This mechanism explains why highly mitotic cells with greater rates of DNA synthesis are more sensitive to RT than cells with low division rates⁽³⁵⁾ such as auditory hair cells.

Fractionation & its rationale

The existence of many “conventional” radiation schedules has been determined by clinical experience and technological advances. The current conventional unit of dose used for radiotherapy is the Gray (Gy), representing the energy absorption of 1 Joule per kilogram ($1\text{Gy} = 100\text{cGy}$; $1\text{Gy} = 100\text{ rad}$)⁽³⁰⁾.

An event that marked a change in the conception of radiotherapy was derived from a study demonstrating that animal sterilization was possible without damage to the skin just by exposing the animal to daily small doses instead of large single doses of radiation⁽³⁶⁾. After this study, the way in which the total dose of radiation was delivered was developed under the concept of fractionation. This concept extended the possibilities of dose delivery from a single dose, to one dose a day (fractionated) and twice a day (hyperfractionated) during 5 days a week for several weeks⁽³⁷⁾. As demonstrated by the previous experiment, the major advantage of fractionation is the sparing of normal tissues.

The effects of fractionation are explained in terms of radiobiological principles, which have been described as the four Rs of radiobiology⁽³⁰⁾. These concepts will be briefly overviewed in the next paragraphs.

The concept of Repair is illustrated by the previous experiment described in testicular sterilization⁽³⁶⁾, showing that fractionation provided a decreased skin damage (more survival) after small fractions were delivered instead of a single total dose.

The principle of Reassortment refers to the radiosensitivity of cells according to their stage and speed in the cell cycle. As previously mentioned, cells with high mitotic

activity are usually more sensitive than resting cells ⁽³⁸⁾. Therefore, organs that depend on the reproduction of the cells such as epithelial organs present early effects when compared to organs with low cellular reproduction (i. e. auditory hair cells).

Repopulation is a compensatory proliferation that occurs after fractionated radiotherapy. Early reacting tissues start repopulation after 2 to 4 weeks after the start of radiotherapy, while late-reacting tissues have minimal proliferation, which implies that the approximated time required for damage to be seen is tissue-dependent ⁽³⁰⁾.

The concept of Reoxygenation refers to the fact that tumors normally have compartments of oxygenated and hypoxic cells; the latter being radioresistant⁽³⁹⁾. Tumors that re-oxygenate efficiently after every fraction are more sensitive to radiotherapy due to the damage-enhancer effect of oxygen in these previously hypoxic cells (Hall and Cox, p. 28)⁽³⁰⁾.

These four concepts explain the basis of fractionated radiotherapy in clinical practice, demonstrating that fractionation is not only effective sparing normal tissue but also enhancing cancer treatment because of the principle of reoxygenation.

Dose and functional damage

The relationship between the dose delivered and damage is commonly demonstrated by cell survival curves where each cell type has a characteristic curve and effect⁽⁴⁰⁾.

One of the most used equations to predict cell survival is the linear quadratic model equation. As described by Isaacson (p. 160) ⁽³⁷⁾, “this equation assumes two cell killing components in radiation: one proportional to the dose and the other one proportional to the dose squared, with survival being represented by S. ...the linear single hit killing component is the parameter α while the quadratic multiple-hit component is the parameter β ”:

$$\text{Logarithm}S = \alpha D + \beta D^2.$$

According to this equation, early responding tissues have a ratio of about 10, while tissues with low α/β ratios are frequently radioresistant and in consequence tend to present late adverse effects⁽³⁷⁾. As an example, the ratio used for cochlear tissue,

which has a late response is about 3⁽⁴¹⁾. This equation is the basis of fractionation strategies in order to keep complications of a specific tissue at minimum when changes to fractionation schemes are performed.

Given that the organ function is related to the proportion of functional cells, it is also practical to obtain curves of organ functional loss versus dose. This is based on the observation of subjects exposed to different numbers of fractions until they present a functional impairment⁽⁴²⁾. With this method, the total dose is then plotted against the probability of a given event to occur. Examples of dose- response curves as complication probability of ear adverse effects are presented in Figure 7.

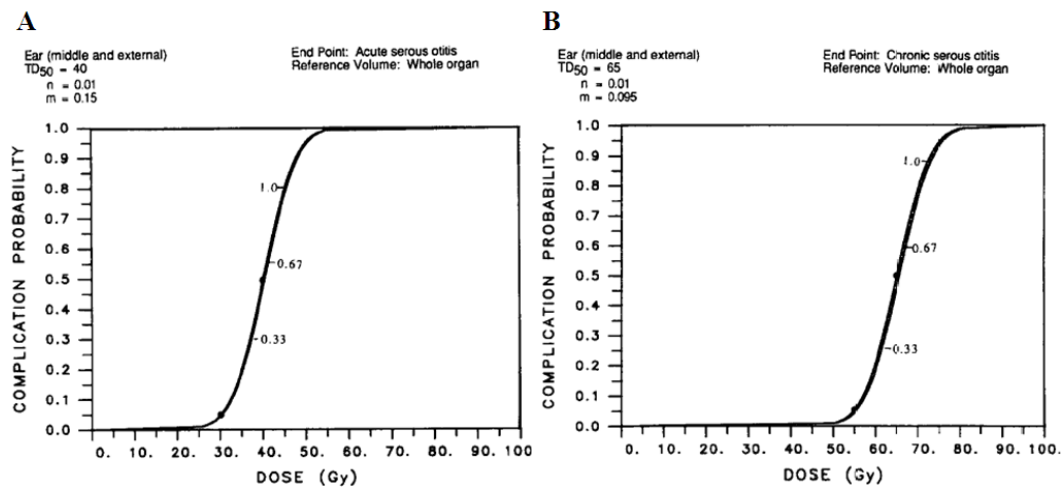


Figure 7. Complication probability of acute serous otitis (a) and chronic serous otitis (b). From Emami B.⁽⁴²⁾ with permission.

While fractionation is used to improve cancer treatment, it also minimizes the effects of radiation in normal tissue. Nevertheless, it does not reduce completely the risk of adverse effects, which can be predicted by the linear quadratic model and complication probability curves. The previously outlined concepts are important in terms of terms of RISNHL and its characteristics which will be discussed in future chapters.

Chapter 2.3. Radiation-induced damage to the ear.

The planning of radiotherapy depends on patient characteristics, technical factors and the specialists involved in the treatment⁽³⁷⁾. The term “conventional radiotherapy” is commonly used; however, most of the treatment protocols tend to vary among oncology centers. For example, with the recent use of intensity modulated radiotherapy (IMRT), the delivery of radiation with sharper beams, the decrease in damage to surrounding normal tissue has become feasible⁽⁴⁾. The next paragraphs will refer to the effects derived from external beam fractionated radiotherapy, which is delivered through a linear accelerator aiming at an organ while the patient is immobilized⁽³¹⁾. Note that the effects that will be discussed are seen when there is direct involvement of the peripheral auditory pathway in the radiation field. This chapter will focus on the parts of the ear that are relevant for the experimental studies to be described.

Radiotherapy & the ear

Radiotherapy can be used in cancer with different purposes such as curative therapy (alone), combined with chemotherapy or following surgical resection of tumors⁽³⁷⁾. In general, the radiation dose for early head and neck cancer ranges from 66 to 72 Gy with a 1.8 to 2.0 daily dose⁽⁴³⁾.

Clinical scenarios where radiotherapy delivers high doses of radiation to the auditory system include stereotactic radiosurgery for vestibular schwannomas and external beam radiotherapy for nasopharyngeal carcinomas, paranasal sinus tumors or parotid tumors⁽²⁾. Furthermore, brain tumors are also treated with focal radiation or whole brain irradiation⁽⁴⁴⁾ which increase the risk of damage to the ear. Despite the advancement in technology, these clinical scenarios still represent a risk of hearing loss when patients are subjected to radiotherapy or in regions of the world where the radiation sources used for radiotherapy are not the most advanced ones.

External ear

As overviewed by Hussey and Wen ⁽⁴⁵⁾, the external ear skin reacts to radiation as skin of other parts of the body demonstrating certain degree of dermatitis with erythema, desquamation and erosion after two or three weeks of fractionated radiotherapy at full doses. However, due to chronic solar exposition, the skin in the pinna tends to be more sensitive to radiation ⁽⁴⁵⁾. Furthermore, exacerbated by ceruminous gland atrophy, the external ear canal can present the previously commented effects, but also can course with necrosis of the cartilage and even stenosis ⁽⁴⁶⁾. These adverse effects can be treated by an otolaryngologist and in most cases represent a cause of transient hearing loss.

Middle ear

Otitis media with effusion is a common complication (up to 50% of patients) after paranasal and nasopharyngeal radiotherapy at total doses ^(47, 48). This complication is secondary to inflammation, accumulation of serous fluid in the middle ear ⁽⁴⁹⁾. In the other hand, the ossicles could be affected by radiation; however, given their tissue composition are in general radioresistant, accounting for few reports of necrosis after treatment ⁽⁵⁰⁾. These complications cause a type of hearing loss that can be managed with low probability of permanent disability.

Inner ear

Radiation induced sensorineural hearing loss has been recognised as a complication after inner ear irradiation; however, it is frequently overlooked by clinicians. Total doses delivered to the inner ear starting from 35 to 40 Gy are known to cause RISHNL for fractionated radiotherapy ⁽⁵¹⁾, affecting initially the high frequency range ⁽⁵²⁾. As will be discussed in a complete chapter of this thesis, this complication cannot be subjected to treatment once that it has been detected.

While complications in the external and middle ear can cause transient hearing loss, RISNHL can be permanent. The characteristics of RISNHL will be discussed in Chapter 2.5.

Chapter 2.4. Methods for audiological monitoring of radiation-induced sensorineural hearing loss.

Audiological assessment can be performed based on direct responses from the patient and by procedures not requiring patient cooperation⁽⁵³⁾. Both types of procedures will be discussed given the relevance for future chapters and in the experiments of this thesis.

Behavioral pure tone audiometry

Pure tone audiometry measures the minimal intensity where a sound of a specific frequency can be detected by the patient at air or bone conduction⁽⁵⁴⁾. While the former involves presentation of the sounds through earphones or loudspeakers, bone conduction refers to the use of a vibrator to stimulate the mastoid process behind the tested ear⁽⁵⁴⁾ in such a way that the sound is detected by means of the auditory nerve, bypassing the external and middle ear.

Thresholds are normally depicted in an audiogram with decibel hearing level (dB HL) in the Y axis versus the frequencies tested in the X axis, usually ranging from 250 Hz to 8000 Hz for air conduction and from 250 to 4000 Hz for bone conduction.⁽⁵⁴⁾

The audiometry method depends mainly on the patient's age. Patients above five years old are asked to give a signal when the tone is heard while younger patients require conditioned playing tasks such moving toys from one place to another when the tone is heard (Comprehensively reviewed by Shoup and Roeser)⁽⁵⁵⁾. By convention, when a patient has elevated air conduction above 25 dB in the range of 500 to 2000 Hz, bone conduction thresholds are obtained to differentiate between conductive problems at the middle ear or sensorineural hearing loss at the inner ear or eighth nerve⁽⁵³⁾. Conductive losses are characterized by elevated air conduction thresholds with normal bone conduction while when there is loss in both, the damage is sensorineural⁽⁵⁴⁾. This method is the most used in the clinical practice as will be seen in the next chapter.

Distortion Product Otoacoustic Emissions

Basically, this test depicts the amplitude of sounds or “echoes” derived from sound-elicited movements of the outer hair cells and the basilar membrane. These sounds are then recorded by a microphone attached to the pure-tone probe in the ear canal⁽¹⁵⁾.

Distortion Product Otoacoustic Emissions (DPOAE) are reduced in amplitude in ears with loss of outer hair cells (Overviewed by Probst, p.189⁽⁵³⁾) (Figure 8).

The DPOAEs obtain their name from the fact that after delivering two tones at the ear (termed as f1 and f2), the cochlea motility creates distorted frequency sounds that travel back (like an echo) and reach the ear canal where they are detected⁽⁵³⁾. For example, a stimulus in the range of 4000 Hz, results in a distorted product in the range of 3200 Hz⁽¹⁵⁾.

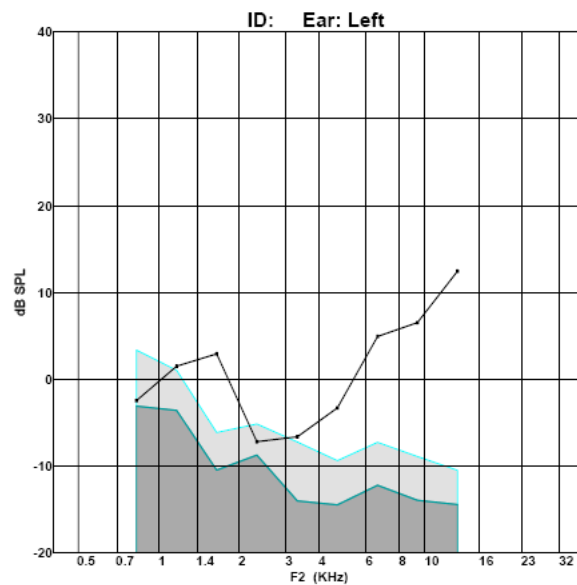


Figure 8. Example of a DPOAE test. Note the reduced amplitude in the lower frequencies compared to the higher frequencies. Shaded areas are the background noise levels. McGill Auditory Sciences Laboratory

Studies have shown that DPOAE amplitude is mainly dependent on the integrity of the outer hair cells⁽⁵⁶⁾. Thus, from a clinical point of view, DPOAE assesses the OHC combined with the endocochlear potential generated by the stria vascularis, which is

needed for the motility of these cells⁽¹⁵⁾. Therefore this test is a good estimate of the integrity of the auditory pathway from the external ear canal to the OHC.

The Auditory Brainstem Response

The ABR is a window of the electrical activity of neurons of the central auditory pathways. This test consists in a series of waves detected after a sound stimulus. The waves are usually plotted in a graph consisting of time in milliseconds (msec) in the X axis and the amplitude (microvolts) in Y axis at different intensity levels (dB)⁽⁵⁷⁾.

Similar to an electrocardiogram, the ABR waves are obtained using an electrode in the earlobe of the stimulated ear and another one positioned at the vertex. A third electrode is placed on the contralateral side serving as ground electrode⁽⁵⁸⁾. With this arrangement the differential electrical activity is recorded following stimuli, resulting in the waves⁽⁵⁷⁾.

Since each peak represents the response from neurons located in the relays of the auditory pathway^(57, 58), most of the knowledge of the ABR has been obtained from experimental studies causing damage to specific points of the brainstem. Most authors agree that wave I represents the response of neurons in the lateral part of the auditory nerve while wave II is originated in the medial part of the eighth nerve⁽⁵⁹⁾. More than one generator has been described for wave III, but the cochlear nucleus has been reported as the principal one⁽²⁶⁾. In the case of wave IV, the SOC has been pointed as the main source. The wave V, which is generated from the lateral lemniscus⁽⁶⁰⁾ and partial contribution of the inferior colliculus⁽⁶¹⁾, is probably the most relevant wave for the ABR.

Since the wave V has a constant shape and has high correlation with behavioral audiometric thresholds⁽⁶²⁾, it is the most analyzed component to determine hearing thresholds⁽⁶³⁾. During testing, as the intensity of the stimulus is decreased the latencies of the waves increase and these become less clear⁽⁵⁸⁾. For these previous reasons, the wave V is used to assess the hearing thresholds in the protocols used in the McGill Auditory Sciences Laboratory (Figure 9).

Two types of acoustic stimulus can be used in the ABR: clicks and tone bursts. The former are pulses of relatively long duration (200 msec) being useful to provide an estimate of hearing sensitivity⁽⁵⁸⁾. However, they cannot be used to assess specific frequencies. For this purposes, tone bursts of specific frequencies with a shorter duration than clicks⁽⁶²⁾ are used⁽⁵⁷⁾. Therefore, the ABR is tool that can be used as screening method or to determine hearing thresholds.

Between the advantages of ABR, include that the test is barely affected by attention, sleep, or sedation contrary to behavioral audiometry⁽⁵⁸⁾. Therefore, the ABR is mainly used in settings such as hearing assessment of newborns, unconscious patients or experimental animals as in this thesis.

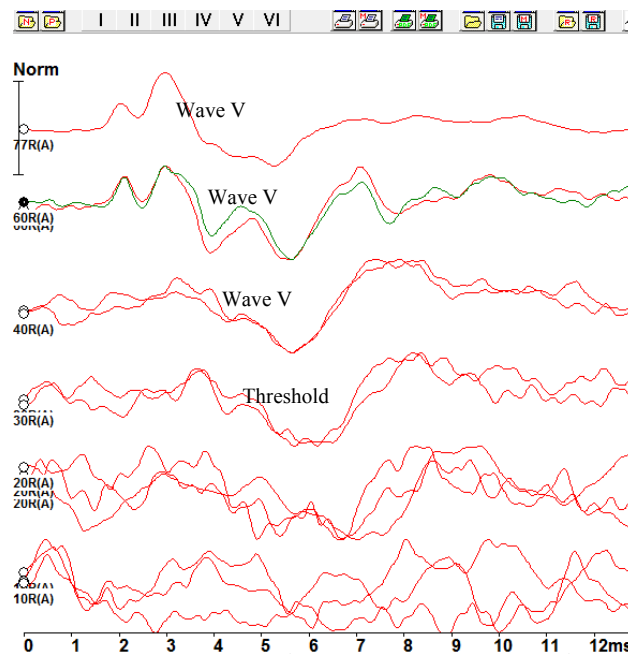


Figure 9. Example of an ABR. McGill Auditory Sciences Laboratory.

While behavioral audiometry requires cooperation of the tested subject, this is not the case for DPOAE and ABR; therefore, the former is relevant for hearing assessment after cancer treatment and the two latter for our *in vivo* experiments using the guinea pig animal model to be described below.

Chapter 2.5. Characteristics of radiation-induced sensorineural hearing loss. A systematic review.

Introduction

The current literature lacks conclusive evidence regarding the incidence and characteristics of hearing loss due to radiotherapy alone as well as its associated risk factors. Articles regarding RISNHL often include patients that are also treated with chemotherapy blurring the degree of hearing loss attributable solely to RT.

The aim of this chapter is to systematically review the literature regarding the incidence, characteristics and risk factors of RISNHL in head and neck (H&N) tumors.

The material derived from this chapter was presented as poster in the American Academy of Otolaryngology Head and Neck Surgery 2012 Annual Meeting and has been accepted for publication as Systematic Review in Head & Neck.

Methods

Search strategy

A systematic review of all scientific articles reporting RISNHL in patients suffering from H&N neoplasms was conducted. All articles published between January 1970 and January 2011 were eligible for inclusion. The search was performed with the assistance of a librarian using seven databases: Ovid MEDLINE, PubMed, Embase, Biosis Previews, The Cochrane Library, Scopus and ISI Web of Science. The search included the following keywords: “radiation”, “radiotherapy”, “radiation therapy”, “irradiation” and “auditory”, “hearing loss”, “sensorineural hearing loss” and “cancer”, “head and neck neoplasm”, “otorhinolaryngologic neoplasms” and their combinations. Complete search strategies can be obtained from the authors.

Criteria for inclusion

Inclusion criteria for the studies were as follows: a) the main focus of the article was on auditory complications following RT in H&N cancer therapy; b) the study

mentioned the incidence of SNHL and c) the outcome measures were obtained following an audiogram with bone conduction threshold measurements. Only literature published in English, French or Spanish were considered. Bibliographies were manually reviewed in order to obtain additional articles of relevance. In publications comparing RT and chemotherapy, the RT alone group of the studies were taken into account.

Reviews, editorials, case reports and articles with non-human data were excluded. Articles describing primary tumors that could affect the auditory pathway, patients receiving concurrent chemotherapy, and articles not describing RISNHL were also excluded. In addition, patients with a mean follow-up period of less than 12 months were excluded because previous publications report a latent period of at least 12 months for RISNHL development ^(64, 65). Whenever selected articles did not report the incidence, the authors of the study were contacted. Articles were excluded if the authors did not respond or were not able to provide the necessary data.

Quality assessment

The eligible articles were assessed for quality using the modified Downs and Black (DB) scale ⁽⁶⁶⁾, as it is a validated checklist for randomized and non-randomized studies. Two investigators independently rated the selected articles in a blinded fashion and scores were then compared using the Pearson correlation coefficient to determine the interrater reliability. A value above 0.8 was considered acceptable for a significance level of $\alpha < 0.05$. For each study, the mean score was calculated and articles scoring below 14 out of 25 possible points were excluded from the review due to insufficient quality.

Results

Search Results and quality assessment

Of 1862 citations identified initially, 44 were selected for complete evaluation. Of these, 24 articles were eliminated as they did not meet the inclusion criteria. Thus, 20 research publications underwent quality control assessment (Fig. 10).

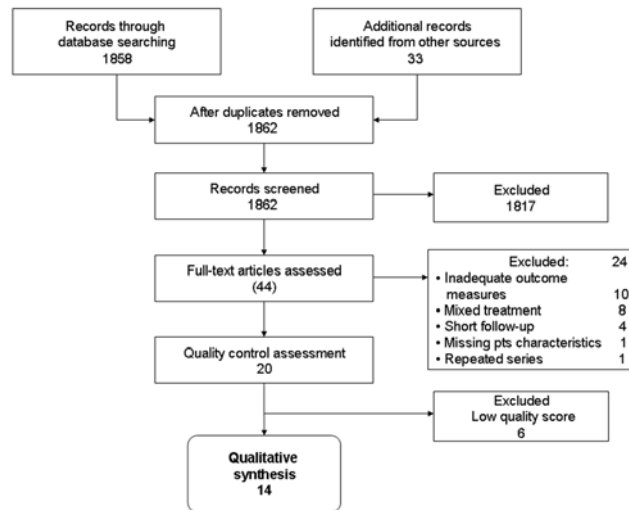


Figure 10. Flow diagram of the search strategy. With permission.

Studies ranged from 7 to 19 out of 25 points on the DB scale. The Pearson correlation coefficient was 0.93 ($p < 0.0001$) indicating strong agreement between reviewers in the assessment. Six articles received a mean score below 14 and were excluded from the final evaluation.

Fourteen research publications were included in the systematic review. Eight were prospective studies^(51, 64, 67-72) and six were retrospective studies^(4, 65, 73-76). All of the publications were observational studies with a level of evidence IV, with the exception of one prospective cohort study (IIb).

Characteristics and Incidence of hearing loss

The incidence of SNHL observed at frequencies above 4 kHz is greater than that observed at frequencies in the speech range (Fig 11). The incidence of SNHL reported for the speech frequencies ($< 4\text{kHz}$) varied from 0 to 85% while seven studies reported the incidence of high frequency SNHL ($\geq 4\text{kHz}$) ranging from 27 to 95%^(51, 67-69, 71, 76) (Table 1). When taking into consideration the reported incidences of all studies, it is noticed that at the shortest follow-up period, greater SNHL is detected at frequencies above 4 kHz (Fig 11a); a trend observed up to the maximal mean follow-up period of 8 years. As the follow-up period increased, an increase in the incidence of SNHL was observed.

Table 1. Selected studies of radiation-induced SNHL in H&N cancer

Author	Study (level of evidence)	Patients	Irradiated organ	Radiation energy and technique	Total dose (Gy)	Fraction dose (Gy)	Follow-up	Incidence (longest follow-up)
Prospective								
Li JJ (2010) ⁽⁶⁷⁾	Case series (IV)	24 (48 ears)	Nasopharynx	MV, 3D	60-65	1.8-2	1, 2, 5 yrs	Average: 60 %, 4 kHz: 97 %, 6 & 8 kHz: 95.8%
Sumitsawan Y (2009) ⁽⁶⁸⁾	Cohort study (IIb)	55	Nasopharynx	MV, 3D	60-76 (mean 69)	2	0.3-17.2 yrs (mean 5.4 yrs)	Average: 85.5 %
Yilmaz Y F (2008) ⁽⁶⁹⁾	Case series (IV)	19 (38 ears)	Various H&N	Cobalt 60, 3D	60-70	2	1 & 12 months	Average: 47%, 4 kHz: 34% 6 kHz: 39%, 8 kHz: 44%
Low WK (2005) ⁽⁷⁰⁾	Case series (IV)	27 (54 ears)	Nasopharynx	6 MV, 3D	66-70	2	3 months, 1.5 & 4 yrs	Average: 29.6 %
Pan CC (2005) ⁽⁵¹⁾	Case series (IV)	12	Various H&N	MV, 3D	40-70 (median 64)	1.8-2	1, 6, 12 months & 2, 3 yrs	4 kHz: 50% 8 kHz: 40%
Wang LF (2004) ⁽⁷¹⁾	Case series (IV)	(89 ears)	Nasopharynx	6 MV, 3D	66-74	1.8-2	2 yrs	Average: 37% 4 kHz: 27%
Leighton SE (1997) ⁽⁷²⁾	Case series (IV)	19 (38 ears)	Nasopharynx	6 MV, 2D & 3D	60-66	2.5	3 & 12 months	0%
Grau C (1991) ⁽⁶⁴⁾	Case series (IV)	22 (43 ears)	Nasopharynx	Cobalt 60, 4 or 8MV, 2D	50-68 (mean 64.7)	>2	7 - 84 months (mean: 2 yrs 9 months)	Average: 21%
Retrospective								
Wakisaka H (2011) ⁽⁷³⁾	Case series (IV)	15 (30 ears)	Nasopharynx	Cobalt 60, 4, 6 or 8MV, 3D	60-70	2	1-12 yrs (median 6.5 yrs)	Average: 26.6%
Chan SH (2009) ⁽⁷⁴⁾	Case series	15 (30 ears)	Nasopharynx	6-MV, 3D, IMRT	50-70	2	2 yrs	Average: 16.7% 4 kHz: 33.3%
Bhandare N (2007) ⁽⁶⁵⁾	Case series (IV)	282	Various H&N	MV, Various techniques	55-81 (median 66.5)	1.3-2	0.5-30 yrs (median: 5.4 yrs)	Average: 13.4%
van der Putten L (2006) ⁽⁴⁾	Case series (IV)	41	Parotid	MV, IMRT	50-70 (mean 64)	1.8-3	2-17 yrs (mean: 6.3 yrs)	Average: 20%
Chen WC (1999) ⁽⁷⁵⁾	Case series (IV)	21	Parotid	MV, 2D	48-70 (median 60.8)	1.8-2	2 -14 yrs (mean: 7.22 yrs)	Average: 43%
Schot LJ (1992) ⁽⁷⁶⁾	Case series (IV)	30	Parotid	8 MV, 2D	38-65	2-2.5	1-14 yrs (mean: 8.1 yrs)	1-2 kHz: 36%, 4-8 kHz: 50% 10-20 kHz: 57%

Abbreviations: H&N, head and neck; MV, megavoltage; 2D, two field technique; 3D, three field technique; IMRT, intensity modulated radiation therapy; Gy, Gray; yrs, years; kHz, kiloHertz.

Since prospective studies have fewer potential sources of bias than retrospective studies, the data was analyzed separately. SNHL detected at all frequencies increased over time and the greatest increase in incidence per year was observed at 4 kHz when evaluating prospective studies only (Fig 11b). This trend was less prominent but still present in retrospective studies.

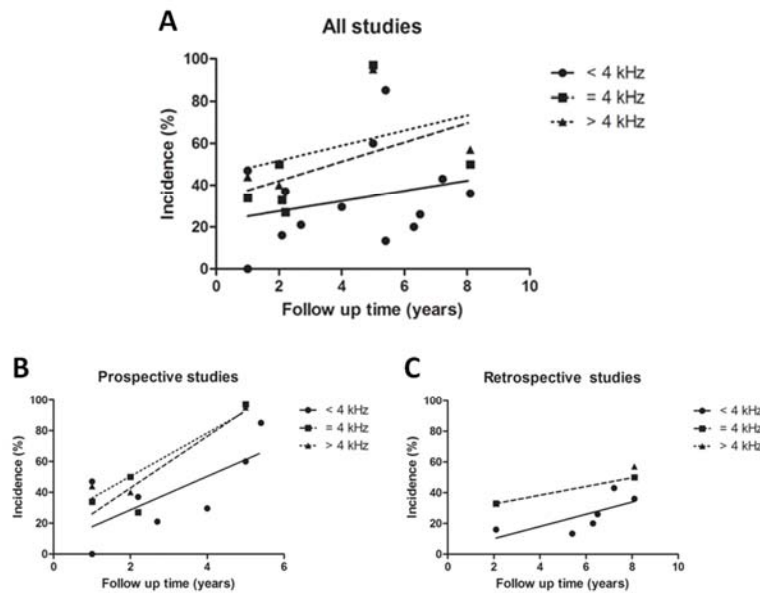


Figure 11. RISNHL is progressive over time. Plots represent the different incidences reported at the latest follow-up of each study as depicted in Table 1. At the longest follow-up period, the incidence of SNHL is greater. With permission.

Two studies included pediatric cases which were pooled along with adult cases of NPC ^(68, 71). Therefore, it was not possible to determine differences in incidence between the adult and pediatric populations. Regarding the primary tumor site, the lowest incidence reported was for cases of nasopharyngeal irradiation ⁽⁷⁴⁾.

Radiation techniques

Only a few studies report on RT using IMRT, which is a technique that has superior normal tissue-sparing capacity (Table 1). The included studies reported most frequently on nasopharyngeal irradiation by a three-dimensional field technique (3D) with the exception of Leighton who described the use of two dimensions ⁽⁷²⁾ and Chan and colleagues who described the use of IMRT ⁽⁷⁴⁾. As for articles regarding parotid

tumors, two describe the use of an ipsilateral two field technique ^(75, 76), and one article refers to IMRT ⁽⁴⁾.

Outcome measures

The outcome measures described in the included articles were heterogeneous. Most of the studies performed the incidence analysis according to the number of ears and few used the total number of patients. Regarding the criteria for diagnosis of RISNHL, the audiometry frequencies evaluated varied between the speech range (<4 kHz) and high frequencies (≥ 4 kHz), the former being the most used for the incidence analysis. The most frequent value used as a significant threshold shift difference in the bone conduction audiogram was 10 dB. However, seven articles considered values of 15 ^(4, 65, 67, 73, 74), 20 ⁽⁷⁵⁾ or 26 dB ⁽⁶⁸⁾.

Risk factors

Table 2 summarizes the risk factors for developing RISNHL mentioned in the eligible studies. Overall, there was a consensus on the total radiation dose administered to the cochlea as the main risk factor. Radiation dose limits to the cochlea, starting from 45 to 60 Gy, were observed to increase the incidence of SNHL ^(4, 51, 64, 65, 74-76). Gender and comorbidities (hypertension, diabetes mellitus) were not found to be risk factors for SNHL development ^(51, 65, 74). The effect of age on the development of RISNHL is inconsistent throughout the reviewed articles.

Discussion

Current treatment protocols for H&N tumors include RT and cisplatin-based chemotherapy, a known ototoxic medication ^(77, 78). As a result, the effects of RT on hearing may be masked by cisplatin-induced ototoxicity since it also leads to SNHL ⁽⁷⁹⁾. With increasing survival rates for patients undergoing chemoradiation, the value of research of auditory complications due exclusively to RT has become eminent. This systematic review has been performed in order to determine the incidence and characteristics of SNHL in head and neck cancer survivors post-radiotherapy as well as discuss possible risk factors involved.

During the evaluation of the eligible articles, inadequate outcome measures were found to be the main source of exclusion. Only articles clearly describing the use of bone conduction audiometry were considered. Whenever articles described the use of the toxicity criteria of the Radiation Therapy Oncology Group (RTOG) / European Organization for Treatment of Cancer (EORTC)⁽⁸⁰⁾ or the Late Effects Normal Tissue Task Force Subjective, Objective, Management and Analytic (LENT/SOMA) scale⁽⁸¹⁾, they were excluded. The RTOG criteria considers subjective hypoacusis as an adverse effect and it does not require the distinction between conductive or SNHL while the EORTC criteria do not include the “ear” as a category of late adverse effects⁽⁸⁰⁾. Thus, clinicians using these criteria may have been inclined to only detect acute auditory toxicities. On the other hand, the LENT/SOMA scale includes objective and analytical evaluation tools⁽⁸¹⁾. However, the use of analytical tools (audiogram) is up to the discretion of the treating physician and varies depending on the treatment center. Thus studies which did not consistently use bone conduction audiometry for screening hearing impairment were excluded from the analysis.

Characteristics and Incidence

Chan et al. described that at least 2 out of 10 patients developed SNHL in the speech frequencies when treated for NPC. Yet, it was observed that at least 3 out of 10 patients developed SNHL in frequencies greater than 4 kHz⁽⁷⁴⁾. A previously published systematic review regarding RISNHL reports a greater incidence at high frequencies as compared to pure tone average measurements. The incidence from pooled data was 42±3 % of SNHL of 10 dB or more at 4 kHz⁽³⁾. However, the authors encountered heterogeneity among studies and therefore pooling of data is questionable.

Various authors have previously described the importance of assessing high frequencies for radiation-induced SNHL^(67, 75, 76). For example, Li et al. reported an incidence of 60% in the speech frequency range and 95% for high frequency SNHL⁽⁶⁷⁾. These results convey three important points. First, as RT-induced

Table 2. Factors associated with risk of developing SNHL		
Author	Factors associated with a greater risk:	Comments:
Li JJ (2010) ⁽⁶⁷⁾	-	High frequency involvement (4-8 kHz).
Sumitsawan Y (2009) ⁽⁶⁸⁾	Age	-
Yilmaz YF (2008) ⁽⁶⁹⁾	-	DPOAE measurement is a good predictor of permanent SNHL. High frequency involvement (6-8 kHz)
Pan CC (2005) ⁽⁵¹⁾	Age Cochlear dose (= 45 Gy) Lower thresholds in baseline audiometry.	Dose-dependent HL at high frequencies (>2 kHz). Gender, diabetes mellitus and/or hypertension did not have a significant effect on HL.
Wang LF (2004) ⁽⁷¹⁾	Age (speech frequencies)	OME post-RT and baseline hearing thresholds did not predict HL. High frequency involvement (4kHz).
Grau C (1991) ⁽⁶⁴⁾	Cochlear radiation dose (= 50 Gy)	Age and baseline hearing thresholds did not predict HL. Incidence of SNHL did not increase with time. High frequency involvement (2-4kHz)
Wakisaka H (2011) ⁽⁷³⁾	Age	Long term HL can occur bilaterally following RT for NPC. Cochlear radiation dose was not influential in the incidence of SNHL. OME post-RT did not have a significant effect on HL.
Chan SH (2009) ⁽⁷⁴⁾	Age (speech frequencies) Cochlear radiation dose (> 47 Gy)	Gender did not have a significant effect on HL. High frequency involvement (4kHz).
Bhandare N (2007) ⁽⁶⁵⁾	Age Cochlear radiation dose (= 55 Gy).	Gender did not have a significant effect on HL.
van der Putten L (2006) ⁽⁴⁾	Cochlear radiation dose (= 50 Gy)	High frequency involvement (4-10 kHz).
Chen WC (1999) ⁽⁷⁵⁾	Cochlear radiation dose (= 60 Gy). OME post-RT	RT-induced HL may be subclinical and dose dependent. Incidence of SNHL did not increase with time. Age was not a predicting factor for developing SNHL.
Schot LJ (1992) ⁽⁷⁶⁾	Cochlear radiation dose (= 55 Gy)	Incidence of SNHL did not increase with time. High frequency involvement (10-20 kHz).

Abbreviations: SNHL, sensorineural hearing loss; kHz, kilohertz; Gy, Grays; OME, otitis media with effusion; RT, radiation therapy; DPOAE, distortion product otoacoustic emissions; HL, hearing loss; NPC, nasopharyngeal carcinoma.

SNHL is progressive, a high frequency audiometry protocol should be consistently performed as a reliable method for early detection and follow-up of patients with RISNHL. Second, given that high frequency SNHL may be subclinical, a selection bias can occur when conducting retrospective studies. Patients aware of their hearing loss may be more willing to participate in the study as compared to patients with no hearing complaints. Third, RT can lead to a decrease in the cochlear reserve. Hence, while patients may not exhibit clinically significant hearing loss, they are at greater risk for future ototoxic insults.

Most of the studies in this review used the pure tone average to report the incidence of SNHL. It is surprising that Leighton et al. reported an incidence of 0% for NPC irradiation ⁽⁷²⁾. The follow-up of 12 months could justify the low incidence observed. Grau et al. reported a latent period of at least 12 months for SNHL development ⁽⁶⁴⁾. Consistent with this result, Bhandare et al. observed a median time interval for SNHL of 2.1 years for patients treated with once-daily fractionation ⁽⁶⁵⁾. The patients reported by Leighton et al. received once-daily fractionation and so, a 12 month follow-up period may be too brief for an accurate evaluation of SNHL incidence. Leighton et al. describe that the absence of SNHL in their case series could be due to the fact that in most of the patients, only the anterior surface of the pons and medulla were irradiated by using a 2 anterior-field technique and that consequently, a lower radiation dose was delivered to the brainstem ⁽⁷²⁾. In addition, the threshold values employed to define SNHL in the audiometric testing were not described in the manuscript and testing at frequencies greater than 4 kHz was not performed.

Raaijmakers et al. demonstrated no statistically significant difference between the incidence of SNHL secondary to RT for NPC and parotid tumors ⁽³⁾. Studies of our review show a tendency of higher incidences of SNHL for cases of nasopharyngeal irradiation ⁽⁷⁴⁾ as compared to parotid region irradiation ⁽⁴⁾. Studies with a higher level of evidence are required to confirm this observation.

Furthermore, radiation technique seems to have an effect on the development of SNHL. A lower incidence of SNHL was observed in studies reporting the use of

IMRT as compared to 2D or 3D techniques. In studies regarding parotid tumors, two articles reported the use of 2D techniques with SNHL incidences of 43 and 36%^(75, 76) while the study by van der Putten et al. reported an incidence of 20% when using IMRT⁽⁴⁾. As for NPC irradiation, the incidence of SNHL reported ranged from 26 to 85% when using a 3D technique^(67, 68, 71, 73). Comparatively, IMRT use resulted in lower incidences (16%), as evidenced by Chan et al.⁽⁷⁴⁾. These results give insight into the enhanced normal tissue sparing capacities of IMRT. Further studies are required to verify this observation.

Outcome measures

In the retrospective studies investigating the effects of parotid irradiation, SNHL was reported according to the values of the non-irradiated ear, which was used as control without baseline measurements. The incidence was therefore determined by comparing the difference of thresholds between ears on every patient. This approach, based on number of patients instead of number of ears, can lead to overestimating the incidence of RISNHL.

In the case of NPC, all of the studies used baseline audiograms to determine the threshold shift differences for each ear separately. The importance of a baseline test for every ear was remarked in the study by Wakisaka et al. which reported that SNHL can occur also in the contralateral side of irradiation for NPC⁽⁷³⁾. The baseline measurement is an important factor when reporting SNHL; it allows the treating physician to determine the degree of hearing prior to RT.

The threshold shift value considered significant to diagnose SNHL varied among studies and ranged from 10 to 30 dB. Studies using greater shift values could have underestimated the actual incidence of hearing loss. Also, the number of consecutive frequencies needed to diagnose SNHL was different among studies, ranging from 1 to 3. These previous limitations can only be overcome by standardizing audiogram protocols as well as elaborating guidelines for reporting hearing loss.

Risk factors

In a study by Honoré et al.⁽⁵²⁾, using the series reported by Grau et al.⁽⁶⁴⁾, an estimated dose-response model for SNHL with risk factor adjustments was constructed. Their results demonstrate that the incidence of SNHL increased proportionally with the radiation dose to the cochlea, while age and low pre-therapeutic hearing level were directly and inversely associated with an increased risk of SNHL respectively⁽⁵²⁾.

Establishing a cochlear radiation dose limit has been challenging. Four review studies have established a limiting dose to the cochlea for SNHL in the range of 35-40 Gy in adults^(2, 82, 83) and 30 Gy in children⁽⁸⁴⁾. Supporting a low limiting dose, are seven of the evaluated articles in this review that mention that greater cochlear radiation doses are associated with greater SNHL. Cochlear radiation dose limits, ranging from 45 to 60 Gy, were reported to be a risk factor for increased SNHL incidence^(4, 51, 64, 65, 74-76).

The studies showed discrepancy in the patient age factor. Given that presbycusis has a prevalence of 35 to 50% in those aged 65 years or older⁽⁸⁵⁾, SNHL can be erroneously attributed to RT in elderly patients. Interestingly, the included studies report patient ages as low as 18 years of age and means around 50-55 years of age. Also, the changes in threshold were evaluated over 1 to 8.1 years (maximum mean follow-up time). Therefore, at these reported ages and for these short follow-up periods, aging is most likely not a contributing factor to the hearing loss reported. The heterogeneity of the patients' age and the lack of reporting threshold values did not allow the authors to perform a comparison with normative historical data to assess the contribution of age in SNHL due to RT.

Only the study by Pan et al. reported the effect of comorbidities on SNHL⁽⁵¹⁾. A logistic regression analysis demonstrated that diabetes mellitus and hypertension did not affect SNHL incidence⁽⁵¹⁾. The interaction between comorbidities, age and RT-induced SNHL remains poorly understood.

Contribution of the retrocochlear pathway

Concerning the assessment of the retrocochlear pathways, conflicting results were observed when both audiometry and auditory brainstem response (ABR) were performed. Four studies employed ABR testing in addition to audiometry to assess hearing ^(64, 67, 70, 72, 86). One study did not detect significant changes in ABR while audiometric testing revealed SNHL ⁽⁷⁰⁾. Li et al. reported prolonged latencies for waves I, III and V at 12, 24 and 60 months as compared to baseline measurements. Statistically significant differences were also observed comparing 12 and 60 months post-RT, therefore demonstrating the progression of SNHL in ABR ⁽⁶⁷⁾. Grau et al. also reported auditory brainstem dysfunction as a result of RT⁽⁸⁶⁾. Interestingly, only 4 out of 9 ears diagnosed with SNHL by audiometric testing revealed abnormalities in the ABR ^(64, 86). As previously mentioned, Leighton et al. justified their results due to decreased radiation dose delivery to the auditory pathways when the radiation was administered with two anterior ports ⁽⁷²⁾. Overall, it seems that the cochlear structures are primarily affected and that retrocochlear structures might be involved to a lesser extent.

Conclusions

With the current evidence, SNHL due to RT is characterized as permanent, progressive and dose dependent. It presents clinically following at least 12 months post-RT with initial involvement of the high frequencies. The impact of age on RT-induced SNHL was inconsistent throughout the articles, while gender was found not to be a risk factor. Further studies are needed to characterize the extent of damage to the retrocochlear pathways and its impact on hearing.

High quality literature regarding SNHL due to RT is lacking. The main source of variability in published articles is the criteria used to define SNHL, which has a direct impact on SNHL incidence reporting. Future studies with standardized outcome measure reporting as well as inclusion of high frequency testing should be adopted using prospective designs. Patients receiving RT should be followed for at least one year after RT with long-term serial audiometry.

Chapter 2.6. Mechanism of radiation-induced sensorineural hearing loss.

After a radiation dose, cochlear cells involved in sound transduction suffer from disarrangement of their homeostasis, which ultimately leads to cochlear dysfunction. In this chapter the mechanisms involved at the cellular and structural levels of the cochlea following a radiation stress will be discussed.

Molecular mechanisms of radiation-induced cochlear damage

Dose-dependent radiation induced apoptosis has already been described in several cells systems and is accepted as a mechanism of cell death *in vivo* ^(87, 88). However, few studies have aimed to specifically investigate auditory hair cells apoptosis. Studies done in auditory hair cell lines OC-K3 were used by Low et al. to study the post irradiation apoptosis and reactive oxygen production⁽⁸⁹⁾. This study made clear that ROS production was increased after 1 hour of irradiation, while the apoptotic cascade marked by p53 activation started 72 hours after the irradiation event. These results evidenced that in radiation-induced cell damage, ROS production is a mechanism preceding the programmed cell death and suggesting that probably is one of the main triggers of it. Downstream the cell death pathway, the activation of p53 is known to induce cell cycle arrest facilitating DNA repair or to undergo apoptotic pathways if irreversible damage has occurred⁽⁹⁰⁾.

Several authors have proposed that the late effects of radiation therapy have been attributed to early inflammation and late fibrogenesis ⁽⁹¹⁾ where reactive oxygen species appear to be also involved^(92, 93). However, it has also been proposed that free radicals not only initiate damage but also propagate the damage by promoting further ROS production in the cell cytoplasm after irradiation ⁽⁹⁴⁾. This postulate is supported by the fact that the ROS production after irradiation is minimal (compared to the free radicals produced by normal cell metabolism), but sufficient to damage DNA in key organelles such as the mitochondria⁽⁹⁵⁾. Since the mitochondria consumes more than 90% of the cell's oxygen, this organelle appears to be the primary site of increased ROS generation after radiation damage ^(7, 96). In support of this idea, Richter et al.

demonstrated that after an episode of irradiation there is a continuous oxidation and mutation rate in the mitochondrial DNA (mtDNA) ⁽⁹⁷⁾. The explanation that the authors proposed was that is probably due to leaking of electrons from the respiratory chain with contribution of the low amount of protective proteins (histones) and less efficient repairing mechanisms as compared to nuclear DNA. This idea was further supported by later experiments of Yakes et al. giving evidence of the higher susceptibility of mtDNA to free radicals compared to nuclear DNA ⁽⁹⁸⁾.

To illustrate the involvement of the mitochondria in ROS production, a study investigated the preventive effect of resveratrol (antioxidant) in mitochondrial DNA damage secondary to ROS production caused by gamma irradiation in larvae of *C. elegans*. Resveratrol decreased the production of ROS and in parallel it maintained the number of unaltered mitochondrial DNA as in control values ⁽⁹⁹⁾. In view of the previous outlined concepts, recent theories suggest that the perturbation of the ROS homeostasis in the long run also contributes to the late effects following radiation ⁽⁹²⁾.

The notion that ROS production promotes late auditory hair cell death could explain why high frequencies (detected at the basal turn of the cochlea) are primarily affected by radiation, which is comparable to other causes of hearing loss such as cisplatin and gentamicin ototoxicity ⁽¹⁰⁰⁾ and noise-induced hearing loss ⁽¹⁰¹⁾, where ROS are directly involved. This effect is attributed due to the lower levels of glutathione, an endogenous antioxidant, in the basal turn of the cochlea as compared to the rest of the turns ⁽¹⁰²⁾. Furthermore, as evidenced by Usami, the outer hair cells have lower levels of glutathione than other cells of the organ of Corti ⁽¹⁰³⁾, and therefore this lower antioxidant capacity make these cells prone to cell death after oxidative insults. Given this parallel mechanism between radiation-induced damage and other causes of hearing loss, it seems that ROS play a triggering role in auditory cell apoptosis after stress.

Evidence from animal models of radiation-induced cochlear damage

In the next paragraphs the main findings derived from animal models of RISNHL with single and fractionated radiotherapy will be overviewed with emphasis on the latter.

Single dose radiotherapy

In the second part of the XXth century, early animal studies assessed the effects of radiotherapy in the auditory system. Novotny ⁽¹⁰⁴⁾ and Kozlov ⁽¹⁰⁵⁾ were some of the first authors to remark the deleterious effects of radiation in hearing. However, the main structure involved in this effect was still unknown. Following studies performed by Kelemen ⁽¹²⁷⁾ demonstrated middle ear effusion and damage to the stria vascularis, suggesting that vascular damage was a key factor in radiation-induced hearing loss. This notion was supported by reports of radiation-induced vasculitis in temporal bones of patients who received irradiation to the inner ear ⁽¹⁰⁶⁾.

Winther further confirmed this findings but also demonstrated cellular and subcellular changes in the outer hair cells of the cochlea ⁽¹⁰⁷⁾ suggesting that the argument of vascular damage had to be extended to understand the effects of radiation in the ear. In addition to his work, other studies have demonstrated a dose dependent hair cell damage using large single doses of RT. For example, Kim and Shin found damage in the OHC and IHC directly after irradiation with doses of 30 and 45 Gy ⁽¹⁰⁸⁾. Evidence linking hair cell damage to RISNHL was given by the study of Tokimoto and Kanagawa who demonstrated a dose dependant degeneration of the OHC in the basal turn of the cochlea, which was correlated with changes in ABR ⁽¹⁰⁹⁾. These studies gave evidence that radiation was damaging mainly the OHC and stria vascularis; however as will be discussed fractionated radiotherapy studies identified that neural structures were also involved in RISNHL.

Fractionated doses

Despite the findings previously mentioned, it is difficult to think that the same structures are involved in damage after fractionated radiotherapy. Single-dose studies

have many drawbacks: the life span of the animals is shortened by the experimental design or by the impending death caused by high radiation doses. Furthermore, preclinical radiation protocols differ from the human ones, providing little insight into the mechanisms of RISNHL in clinical scenarios.

Experiments in chinchillas with fractionated radiotherapy (2 Gy per day up to 40 to 90 Gy) have demonstrated dose-dependent auditory hair cell degeneration in the absence of damage to the stria vascularis even up to 2 years post-irradiation ⁽¹¹⁰⁾; findings that contrast with the results of studies using single-dose radiotherapy.

Theoretically, given that neurons are cells with no capacity of cell division, the spiral ganglion cells are believed to have greater resistance to damage by radiation ⁽¹¹¹⁾. This might explain the fact that in single-dose studies, neuronal damage is less apparent whereas in fractionated radiotherapy, neuronal cell count is decreased after a long term evaluation ⁽¹¹⁰⁾. Nevertheless, the involvement of neural structures in RISNHL is controversial given the findings in clinical studies. For example, a study assessing ABR in NPC patients treated with conventional RT and who developed sensorineural hearing loss, showed no statistically significant difference in the pre and post RT interval wave I-V latencies after one year of follow-up ⁽⁷⁰⁾. Therefore, the involvement of spiral ganglion neurons is still subject of controversy.

Evidence suggests that ROS production in the cells is a triggering factor after radiation, which ultimately promotes cell death if damage is irreversible. However, the damage caused to DNA can have long lasting effects responsible for the late effects of radiation as seen in the cochlear structures.

The evidence from preclinical models suggests that in single doses of radiotherapy, the vascular structures and the hair cells are mainly affected, whereas in fractionated radiotherapy, the auditory hair cells and the spiral ganglion neurons also play a role in the physiopathology of RISNHL. Therefore, as explained by Low ⁽⁶⁾, “in the clinical setting of fractionated radiotherapy, a patient may experience hearing loss when a critical mass of hair cells is lost, months or years after radiation exposure”.

Chapter 2.7. Radioprotection and radiation-induced cochlear damage.

The radiation-induced mechanisms of cell death in the auditory system have implications for attempts to attenuate or prevent hearing loss. Since apoptosis is at the end of the cellular response to radiation a downstream inhibition may not be enough to block cell death ⁽⁶⁾. However, intervention on early stages of cochlear damage such as the production of ROS, which is an initial trigger of cell death, remains promising.

In this chapter the concept of radioprotection will be presented, along with a brief overview of the attempts performed so far to prevent RISNHL in preclinical models.

Radioprotection

This concept refers to any compound that can inhibit or at least decrease the effects of radiation in normal tissue. It is reasonable to think that for more efficiency, the radioprotective agent should be present at the greatest tolerable concentration in the tissue before the radiation dose is delivered. Given the ear anatomy and based on a ROS-dependant model of radiation-induced cochlear damage, systemic and topical radioprotectors can be considered in the arsenal against RISNHL.

After witnessing the destructive potential of the atomic bomb in the Second World War, research was focused in radioprotection. The first compound to demonstrate radioprotective properties was cysteine⁽³⁰⁾. Experiments demonstrated that this compound increased survival in mice subjected to whole body irradiation when compared with non-treated animals⁽¹¹²⁾. After this discovery intensive research was performed to discover other radioprotective agents. However, toxicity was a discouraging event in most of the compounds found ⁽³⁰⁾.

Amifostine is an example of a radioprotector, which has been approved to prevent xerostomia after parotid irradiation ⁽¹¹³⁾. After being metabolized into its active compound, it penetrates the cell by diffusion where it scavenges ROS generated by ionizing radiation⁽³⁰⁾. Interestingly it has a slower absorption in tumor cells. These

characteristics make it ideal for its use as a radioprotector. Despite its promising effect in the salivary glands, amifostine is unable to cross the blood brain barrier⁽¹¹⁴⁾, as consequence, its use in the central nervous system is limited .

Models of radiation-induced cochlear damage & radioprotection

Only a few *in vitro* studies have attempted to test potential radio-protective agents. For example, N-Acetylcysteine has demonstrated to protect auditory hair cell lines after single doses of 20 Gy⁽¹¹⁵⁾. However, no animal study has been performed to confirm its properties *in vivo*. This step is not easy to achieve as will be discussed in the next paragraphs.

Two of the main criticisms of animal models used in RISNHL are lack the clinical scenario of a neoplastic condition (which is reasonable since RISNHL has a late onset and short survival of the animals would preclude long term hearing assessment) and also the lack of a fractionated radiotherapy scheme. To illustrate these, an animal study claimed that amifostine had radioprotective effects against radiation-induced cochlear damage after single doses of 3.5 Gy. The group treated with amifostine showed lower OHC damage compared with RT alone after 1 month post exposure⁽¹¹⁶⁾. Despite these results and according to what is known about RISNHL, there is little evidence to support that damage to the cochlea can actually be caused at this dose or at this time point.

Contrasting with the previous example, studies have used large single doses of radiation to assess potential radioprotective agents. Yang evaluated the effect of extracts from *Radix salvia* by delivering a large single dose of gamma radiation of 60Gy to the guinea pig cochlea⁽¹¹⁷⁾. The limitation of this study is the large single dose used to induce damage, which does not resemble the current clinical practice.

Another research group have attempted to use a fractionated scheme of radiotherapy to test radioprotective agents. Using the α/β ratio for late responding tissue Altas applied a fractionated total cranial irradiation of 6.6 Gy/day for 5 days to determine the radioprotective properties of piracetam⁽⁴¹⁾ and L-Carnitine⁽¹¹⁸⁾. Both compounds showed radio-protection as determined by morphological analysis of light

microscopy. This was a more rational approach in the delivery of radiation; however, the results were based in qualitative evaluation of histological slides and after 4 days of follow-up, which make these results difficult to apply in the human counterparts.

At present there is only one study with evidence of radioprotection in the cochlea. Epicatechin, a compound obtained from green tea, was tested *in vitro* and in two animal models of radiation-induced damage after single doses of radiotherapy (20 Gy). In cell culture, epicatechin promoted a decrease the radiation-induced ROS production, enhancing cell survival; while in the zebrafish and rat model it inhibited radiation damage and ototoxicity respectively ⁽¹¹⁹⁾. Despite that this study has some of the limitations previously discussed; it gave functional and morphological evidence across different experiments supporting the idea that epicatechin can be used as a radioprotector. Nevertheless, no further evidence has been reported about epicatechin and RISNHL.

As seen in these previous paragraphs, there is a need for radioprotective agents that do not interfere with cancer treatment and that are able to reach vital structures such as the central nervous system. Furthermore, in current experiments of radioprotection in RISNHL, the lack of a reliable animal model makes the results of the current literature difficult to reproduce and extrapolate in human scenarios. In Part three of this thesis, dosimetric methodologies will be discussed since it is a key limitation found in the above literature review.

Chapter 2.8. Metformin

The search for a reliable radioprotector in the ear is extremely challenging not only by the difficulties of a reproducible animal model of RISNHL, but also due to limitations regarding the safety of the compound to be used and the potential interference with cancer treatment. As will be overviewed below, the characteristics of Metformin have made it interesting to be tested as a radioprotector.

Characteristics of Metformin

Metformin is a widely used drug in the treatment of type 2 diabetes mellitus. Given its common use in this disease, most of the known effects are derived from studies in diabetic patients. For example, studies have shown that the oxidative status of diabetic patients taking Metformin (determined by the generation of ROS, as well as oxidized protein products) was improved as compared to patients not taking this medication⁽¹²⁰⁾. This suggests that Metformin can have antioxidant properties or that it can regulate the production of ROS during stressing conditions.

At the cellular level, these beneficial effects of Metformin have been associated with the activation of the adenosine monophosphate protein kinase (AMPk), which is a metabolic regulator with a variety of responses including inhibition of the release of inflammatory mediators, promotion of cell cycle arrest and apoptosis (Fig. 12)⁽¹²¹⁾.

The characteristics that make Metformin an interesting agent to be tested as a radioprotective agent include the following: 1) it is a medication that has an oral bioavailability of approximately 60%, exerting its effect without being metabolized into secondary compounds⁽¹²²⁾; 2) its main adverse effect is lactic acidosis, which usually presents under renal insufficiency⁽¹²³⁾; 3) It has the peculiarity of being accumulated in cells that are rich in mitochondria, the main producer of ROS⁽¹²⁴⁾ (most importantly, for the mechanism of radiation-induced damage); 4) Metformin crosses the blood-brain barrier^(125, 126), which is an important characteristic if it is intended to be used as a radioprotector when central nervous system tumors are being irradiated and 5) It is up taken by nephrons through the organic cation transporter 2

(OCT2),⁽¹²⁷⁾ which has also been reported to be found in cochlear structures⁽¹²⁸⁾. Considering all of these characteristics, we could hypothesize that Metformin can reach the organ of Corti and be taken up by the structures involved in sound transduction without causing adverse effects.

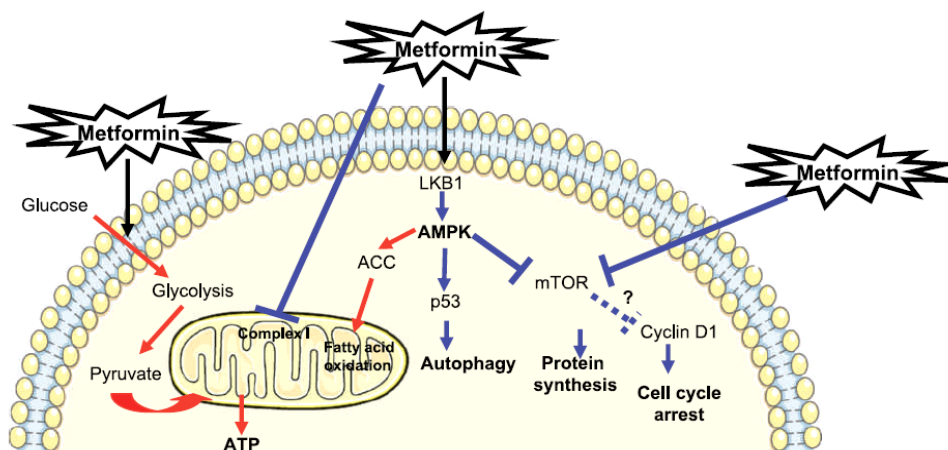


Figure 12. Proposed mechanism of action for Metformin. From Ben Sahra et al⁽⁹⁾ with permission.

Metformin as a reactive oxygen species regulator

As outlined in previous chapters, ROS are important triggers of cell death following irradiation, therefore the question is whether Metformin can scavenge or reduce ROS. In the next paragraphs this question will be discussed.

Early studies using gamma rays in water to create ROS and free radicals, demonstrated that Metformin decreased the production of free radicals in hypermetabolic cells⁽¹²⁹⁾. Nevertheless, in another study of the same research group, it was found that Metformin had minimal ROS scavenging activity⁽¹³⁰⁾. This evidence suggests that Metformin acts mainly through an intracellular mechanism to regulate the production of ROS (Reviewed by Ben Shra⁽⁹⁾).

Further studies have proposed that the main mechanism of Metformin is the inhibition of the respiratory chain in the mitochondria, reducing the production of ROS⁽¹³¹⁾. Cell culture studies have rejected the idea of scavenging properties and gave evidence of the intracellular metabolic regulatory effect of Metformin. When hydrogen peroxide

(H₂O₂), an external source of ROS, was applied to embryonic fibroblasts, Metformin was unable to reduce ROS production due to this stressor⁽¹³¹⁾, which rejected the idea of a direct scavenger property and supports the intracellular mechanism.

In addition to the previously findings and with high relevance for this thesis, experiments have demonstrated that Metformin prevented oxidative stress induced-cell death in cortical neurons⁽¹²⁾. Furthermore, *in vitro* studies in cochlear auditory hair cell lines confirmed that Metformin increased survival after the administration of gentamicin (an ototoxic drug) by reducing the ROS production⁽¹⁴⁾. In view of the previous evidence, the hypothesis for this work is that Metformin can prevent RISNHL secondary to the inhibition of ROS formation in the cochlear cells.

Metformin as an anticancer agent

As previously mentioned, the studies in diabetic patients, also served to identify the anticancer effects of this compound (reviewed by Ben Sahra⁽⁹⁾). A large prospective study found that patients receiving standard doses of Metformin were at lower risk to developing cancer as compared to diabetics without any use of Metformin in their medical history⁽¹³²⁾. Stronger evidence was derived from more specific studies where subgroups of diabetic patients with cancer were recruited. For instance, a study analyzed breast cancer response to chemotherapy in a control group and two subgroups of diabetic patients taking and not taking Metformin respectively. Interestingly, a higher survival rate was seen in diabetic patients taking Metformin as compared to the rest of the groups⁽¹³³⁾.

The consistent findings among different independent studies led to a wave of intensive research on cancer models confirming the effects of Metformin previously discussed. Animal studies consolidated the notion of Metformin as an anticancer agent demonstrating that it prevented the development of breast and colon tumors in genetically-modified mice predisposed to cancer^(134, 135). In terms of direct cancer treatment and more importantly for the head and neck area, Metformin has been reported to inhibit the growth of cell lines derived from head and neck squamous cell carcinoma⁽¹⁰⁾. Studies with an *in vivo* model, confirmed the previous results, showing

that a diet with supplemented Metformin reduced the growth of lung cancer in animals when compared with a non-supplemented diet ⁽¹³⁶⁾. Therefore, patients with head and neck cancer could benefit from Metformin's effects during their treatment.

Metformin and its interference with radiotherapy

Despite the previously commented evidence, the question whether Metformin can interfere with radiotherapy treatment by protecting cancer cells arises.

As previously mentioned, AMPk is the main protein involved in the effects of Metformin. One of its functions includes the activation of p53, promoting cell cycle arrest, inhibiting energy consumption ⁽¹³⁷⁾ and reducing the production of ROS. It is hypothesized that through this mechanism, Metformin has differential effects on cancer and normal cells. Moreover, it has been reported that tumoral cells with a p53-deficient system lack normal metabolic pathways making them unable to undergo the energetic adaptation forced by Metformin, making this drug selectively toxic to these cells ⁽¹³⁸⁾.

Studies have demonstrated that AMPk plays a major role in survival of cells subjected to radiation. The study compared the survival of normal and AMPk knockout fibroblasts following irradiation. Interestingly, fibroblasts were only able to proliferate in the presence of a functional AMPk ⁽¹³⁹⁾. In the cancer counterparts, a cell culture study demonstrated that Metformin enhanced the AMPk activation after irradiation, promoting cell death. Moreover, it also demonstrated that the inhibition of AMPk provides resistance to cancer cells against irradiation ⁽¹⁴⁰⁾.

Summarizing the previous evidence, the beneficial effects of AMPk activation on normal cells, its effects on cancer, and its potential availability in the inner ear support the idea of Metformin as a potential agent that could improve the treatment of tumor cells while preventing the damage of normal cells. These characteristics make Metformin an interesting agent to evaluate in order to prevent radiation induced late hearing loss.

PART THREE: Experimental studies

Chapter 3.1 Introduction & overall experimental plan.

In view of the literature review presented in Part two, there is a need to determine whether Metformin is radioprotective. This will be done using both *in vitro* and *in vivo* studies.

The *in vitro* studies will be done using cell culture experiments with a cochlear cell line in a 3 arm study. The first arm (radiation lethal dose) will estimate the half-lethal dose; the second arm (Metformin lethal dose) will estimate the cytotoxicity of Metformin; finally the third arm (Metformin and radiation) will evaluate whether Metformin is radio-protective.

The *in vivo* study will have two phases. The first one will do preliminary experiments to determine how to best deliver an accurate dose to the guinea pig cochlea using unilateral irradiation. The second and main phase will use the results of the first phase to deliver a scheme of fractionated radiotherapy to the guinea pig cochlea to ultimately evaluate whether Metformin is radioprotective.

Chapter 3.2. In vitro estimation of the cytotoxic and radioprotective effects of Metformin.

Introduction

This chapter will evaluate whether Metformin is cytotoxic and radio-protective using an auditory cell line in the 3-arm in vitro study outlined above.

Objective

To estimate the cytotoxic and the otoprotective effects of Metformin against radiation-induced damage in an isolated auditory hair cell line.

Methods

With modern tissue culture techniques, it is possible to obtain cell lines from many different tissues and tumors. Isolated auditory hair cell lines are useful for the screening of potential ototoxic and otoprotective agents. In addition, they help to delineate the molecular and cellular events involved either in cell death or otoprotection depending on the agent tested.

The HEI-OC1 Cell line

The House Ear Institute-Organ of Corti 1 (HEI-OC1) cells are obtained from transgenic mice (Immortomouse - Charles River Laboratories). While the mouse organ of Corti becomes functional 12 to 14 days after birth, this cell line is obtained from cochlear turns from mice at postnatal day 7⁽¹⁴¹⁾. When cultured in permissive (33°C) and non-permissive conditions (39°C), this cell line expresses the neuroepithelial cell marker Nestin as well as cell markers of sensory and supporting auditory cells such as Math 1, Myosin VII, Prestin, OCP2 and Connexin 26⁽¹⁴²⁾.

This cell line has been reported to be sensitive to ototoxic drugs⁽¹⁴²⁾ and has been used in experiments involving radiation induced auditory cell damage⁽⁸⁹⁾. Therefore, this cell line is used as a screening tool for ototoxicity of new pharmacological drugs and for investigating the cellular and molecular basis of ototoxicity.

Irradiation system

Ninety-six-well plates were positioned inside the Faxitron CP-160 Cabinet X-Radiator System (Faxitron X-Ray Corp., Wheeling, IL, USA) on tray guide #6 (source to surface distance of 43.2 cm). Added filtration used was a 0.5 mm Cu filter and the beam parameters were set at maximum (160 kVp at 6.3 mA). All the irradiations were programmed with a dose rate of 0.5 Gy per minute and varying the exposure time accordingly to the desired dose administered.

Cell culture

HEI-OC1 cells were generously provided by Dr. Kalinec from House Research Institute, Los Angeles. These cells were cultured under permissive conditions (33 °C and 10% CO₂) and maintained as monolayer cultures in high glucose Dulbecco's Modified Eagle Medium (DMEM; Life Technologies, Canada) supplemented with 10% fetal bovine serum (FBS; Wisent, Canada) without any antibiotic treatment.

Cells were seeded in ninety-six-well plates at a density of 4000 cells/well in 200 µL DMEM and left to attach for 24 hours. The cells were then treated when they became at least 70% confluent with the following scheme:

Experiment 1. Lethal dose of radiation: The cells were exposed to various doses of radiation (0–30 Gy) to obtain a dose curve and the dose at where 50% of the cells survive compared with non-irradiated plates. The 3-(4, 5-dimethylthiazol-2-yl)-5-(3-carboxymethoxyphenyl)-2-(4-sulfophenyl)-2H-tetrazolium (MTS) assay was conducted after 48 hours to monitor the cell viability.

Experiment 2. Lethal dose of Metformin: The cells were incubated with different doses of Metformin (0 - 5mM) for 48 hours. Subsequently, the MTS assay was performed to monitor cell viability. This experiment served to determine the cytotoxic dose of Metformin on HEI-OC1 cells.

Experiment 3. Metformin and radiation: The cells were incubated with different doses of Metformin (0 – 5 mM) for 24 hours and irradiated thereafter using the radiation dose at which 50% of the cells survived (15 Gy). After 48 hours of incubation at 33

°C, the MTS assay was used to determine whether Metformin can protect HEI-OC1 cell against radiation.

Cell viability test: MTS assay

The MTS assay is based on the reduction of MTS compound into a colored product by NADPH or NADH, which is produced by dehydrogenase enzymes in metabolically active cells⁽¹⁴³⁾. This test was performed according to MTS assay kit operating protocol (Promega Corporation, Madison, USA). Twenty five microliters of MTS assay solution were added to each well and the cells were incubated at 33 °C for 90 minutes. The metabolic activities of cells were recorded as relative colorimetric changes, measured at 490 nm using a microplate reader (Biotek, USA).

Statistical analysis

Comparison of the means of different groups was completed using one-way analysis of variance (ANOVA). Where data were derived from 3 independent experiments, the parameters were expressed as the mean \pm standard deviation (SD). Post-hoc Dunn test was used for pair-wise comparisons of results found to be significant by repeated measures of ANOVA. Statistical significance was inferred at $p < 0.05$.

Results

As shown in Figure 13, radiation decreased the viability of the HEI-OC1 cells in a dose-dependent manner. By creating a dose response curve, we could infer that the dose needed to decrease cell viability in 50% was approximately 15 Gy. Therefore, this dose was chosen for future radiation experiments in cell lines.

When applying different Metformin concentrations to the HEI-OC1 cells, none of them were proven to be ototoxic following 48 hours. The highest Metformin concentration tested (5mM) caused a decrease in 10% of cell viability. No statistically significant differences were found between the different concentrations (Figure 14).

The effect of various concentrations of Metformin was examined on the radiation-treated cells and it was discovered that Metformin did not protect the HEI-OC1 cells from radiation-induced cytotoxicity in a dose-dependent manner. There were no

statistically significant differences between the cells radiated with 15 Gy and the cells treated with Metformin before radiation (Figure 15).

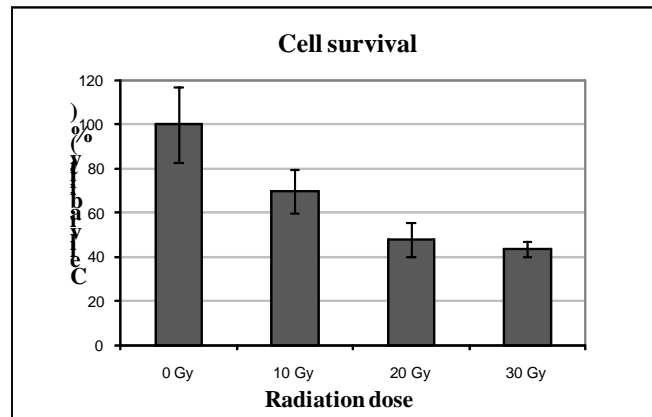


Figure 13. Radiation decreased cell viability. The data represent mean + standard deviation.

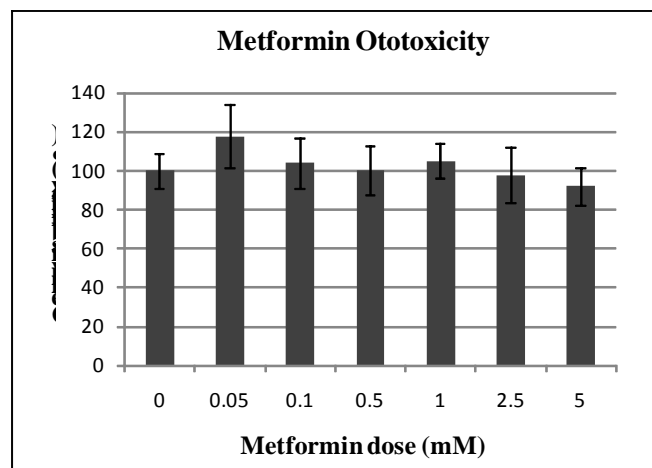


Figure 14. Metformin LD50. The data represent mean \pm standard deviation.

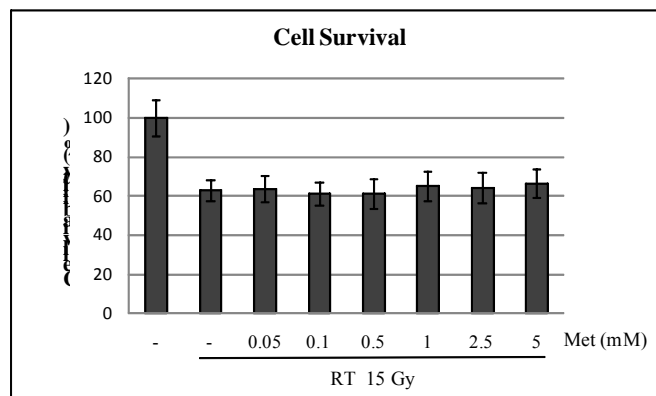


Figure 15. Metformin (different doses) and Radiation-induced (15 Gy) auditory cell death. The data represent mean \pm standard deviation.

Discussion

The present study investigated the otoprotective effect of Metformin against radiation induced cochlear damage. *In vitro* experiments demonstrated that Metformin does not have deleterious effects in a cochlear cell line. Even at high doses such as 5 mM (which are 100 times the concentration of doses achieved in prescribed doses to diabetic patients⁽⁹⁾), Metformin demonstrated a slight decrease in cell survival which was not statistically significant from control plates.

Concerning the otoprotective effect of Metformin *in vitro*, cell survival after radiation was not affected by the addition of Metformin. Metformin did not provide protection against radiation-induced cell damage. Nevertheless, it was found that Metformin also did not radiosensitize the cell line, which confirms its safety in normal tissues during radiotherapy treatment.

A limitation of *in vitro* studies is the fact that they lack the complete cochlear environment - missing important structures involved in the process of hearing such as the stria vascularis, differentiated spiral ganglia neurons and the ionic composition of the cochlear fluids. Thus it was decided to continue the *in vivo* experiments.

Conclusion

Metformin was not ototoxic or radio-protective radiation-induced auditory hair cell damage *in vitro*.

Chapter 3.3. Methodology for controlled radiation of the guinea pig cochlea

Introduction

The search for a reliable radioprotector in RISNHL is a growing field; however as previously discussed most of the preclinical research is missing a reliable and reproducible animal model of RISNHL.

Most of the small animal irradiation systems use energy sources in the kilovolts (kV) range, whereas current human radiotherapy units use megavolt (MV) photon beams. These are known to be unsuitable for irradiating small animals. For MV photon beams the extent of dose buildup gradient is around 1-2 cm, which in some cases is of the order of the animal size itself, and therefore the delivery of uniform doses to target structures in small animals becomes challenging ⁽¹⁴⁴⁾. While kV radiation systems are more readily preferred for animal RT, one has to keep in mind that kV energies lead to an increased dose absorption in bone tissue due to a photo-electric effect ⁽¹⁴⁴⁾. Therefore, since the organ of Corti is enclosed within the temporal bone, the dose delivered to the auditory cells is directly affected by the type of energy used and by the beam direction through the cochlea.

For these previous reasons, setting-up a small animal irradiation protocol of fractionated cochlear irradiation is of a particular challenge. Winther proposed a guinea pig model allowing irradiation to one ear while the contra lateral ear received negligible radiation doses ⁽¹⁰⁷⁾. This model has been subjected to different modifications in terms of energies, radiation fields (collimators) characteristics and furthermore has reported contradictory outcomes ⁽¹⁴⁵⁾. Preclinical studies of radiation-induced cochlear damage often do not consider dose measurements at the cochlear plane and also ignore photon scatter and beam energies. In most of the cases, this makes the outcomes of the studies difficult to reproduce. Therefore it is important to develop a reproducible dose verification approach that enables comparability between animal studies given their potential clinical relevance.

Radiochromic films contain a sensitive layer that in the presence of radiation reacts to form a blue colored polymer, showing the distribution of radiation according to the intensity of staining⁽¹⁴⁶⁾. Compared to thermoluminescent dosimeters (TLD's) or ionization chambers, the radiochromic films are a much more advantageous option to consider due to their lower cost, ease of handling and utility in small spaces. The spatial resolution and low spectral sensitivity of radiochromic films make them ideal for the measurement of dose distributions in regions of high dose-gradient radiation fields⁽¹⁴⁷⁻¹⁴⁹⁾.

Objectives

In view of the above, this preliminary *in vivo* study aimed to describe a method to perform planning and dosimetry for an animal model of radiation-induced cochlear damage using radiochromic films and compare it to previous methods reported in the literature. The use of films had two objectives. The first was to give an ideal irradiation field size for unilateral cochlear irradiation while avoiding irradiating the mid-brain and contra-lateral ear at harmful doses in guinea pigs. The second objective was to demonstrate the need to deliver known doses of radiation to real tissue instead of tissue substitute materials (phantoms) to give a more accurate estimate of the radiation dose received by the inner ear in future experiments.

Methods

Animal model and restrainer

A female albino guinea pig (500 grams) with normal ear anatomy was placed in a customized restrainer constructed from the original design described by Winther⁽¹⁰⁷⁾. The device allowed a protective lead shield to be used under a radiation source. The front teeth of the guinea pig serve to suspend the head from a horizontal 1 mm diameter wire while two opposing lateral screws keep the animal's head immobile. The collimator with a hole for the irradiation field was supported by the walls of the restrainer and placed on top, covering the entire animal with the exception of the region to be irradiated. The study was approved by the McGill University Animal Care Committee.

CT scan imaging

The guinea pig was anesthetized with an intramuscular injection of ketamine (50 mg/kg) and xylazine (9 mg/kg). The animal was placed in the restrainer with the exact position for planned radiation experiments. The collimator was changed for a polyvinyl chloride (PVC) slab on top of the restrainer and CT scan images (2 mm slice-thickness) were obtained from the whole setup. Reconstruction and target volumes were created within Selection Workspace of the Soma Vision simulation software (Varian Medical Systems, Palo Alto, CA). The cochlea and the planning target volume (irradiation field) were defined using the basal and the apical turns of the left cochlea to guide delineation in reconstructed images (Figure 16).

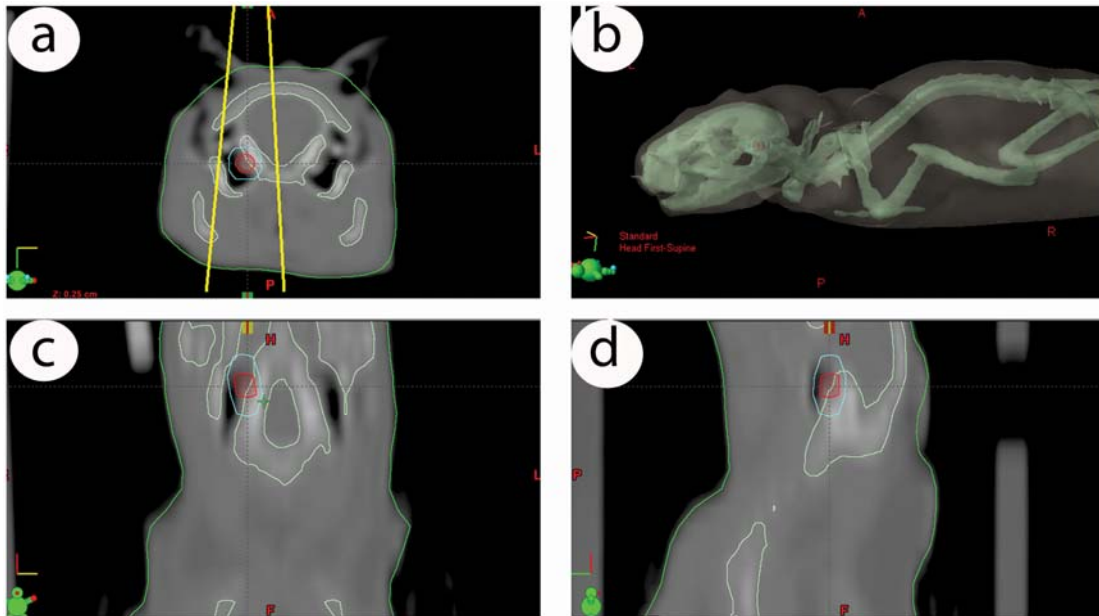


Figure 16. Localization of the guinea pig cochlea in CT scan images (a) and reconstruction of the cochlear volume (b); simulation in reconstructed images was performed to locate the cochlear volume and the irradiation field(c). A confirmatory CT scan with the final irradiation field revealed the adequate positioning of the collimator over the cochlea (d).

With the cochlear volume localized, coordinates and distances of the cochlea in the three dimensional space from the bottom and upper part of the animal body were registered. The guinea pig cochlea had its largest width measurement in the basal turn of 3.5 mm and 5 mm at its main axis (modiolus). The cochleae were located at 15 mm

depth from the skin having the modiolus oriented perpendicular to the beam's direction. According to CT images and external landmarks, the second turn of the cochlea was located at the level of the external acoustic meatus and 4 mm lateral from the midline. In addition distances to the contra-lateral cochlea were taken.

Phantom construction

Phantoms of the guinea pig head were constructed using the measurements of the CT images with a mold of 8 x 12 cm long.

Phantom 1. A single material phantom was constructed similar to the original used by Winther⁽¹⁰⁷⁾. It was decided to use PVC because this has been used as tissue substitute material in other radiation dosimetry studies⁽¹⁵⁰⁾. A phantom made out of two 15 mm thick slabs was constructed (Figure 17a). An additional 6 cm long and 2 cm thick slab was added at the bottom-rear part of the phantom, to simulate the animal's head being suspended by the teeth holder of the restrainer. The modiolus was represented in the space between the two parts of the phantom (15 mm depth) as in the real animal. Taking as reference the measurements in the CT scan, marks in both pieces of the phantom were placed at the vertical level of the left cochlea. The cochlea was marked according to its location in live animal at 47 mm from the anterior border. In this phantom the experiments to decide the irradiation field were performed.

Phantom 2. Measures in the CT images were made to determine the thickness of the bone that the beam traverses in its way to the second turn of the cochlea. Since Teflon is commonly used as tissue substitute material of bone⁽¹⁵¹⁾, a correction equation between the bone and Teflon densities was used to define the thickness of the Teflon slabs needed in order to obtain equivalent bone dose absorption as in the animal. The upper part of the phantom was constructed with slabs of different thicknesses (4 mm PVC-skin and subcutaneous tissue, 5 mm Teflon-cranial cortical bone, 2 mm PVC-brain tissue, 5 mm Teflon-temporal bone tissue and cochlea), whereas the lower part was adjusted for thickness (2 mm of Teflon-cochlea, 20 mm PVC-mandible and thorax (Figure 17b).

Frozen animal. After confirmatory CT scan of the final irradiation field, the animal was euthanized, positioned properly in the restrainer and kept frozen at -24 °C for 48 hours. After this period the animal was removed from the restrainer and the mandible was sectioned leaving a flap with the lower portion of the animal body inferiorly and the exposed cranial base superiorly in order to leave enough space to position a chromic film between the two portions. The floors of both tympanic bullas were removed to see both cochleae completely. This allowed placement of the animal in the restrainer with a film directly below both cochleae (Figure 17c).

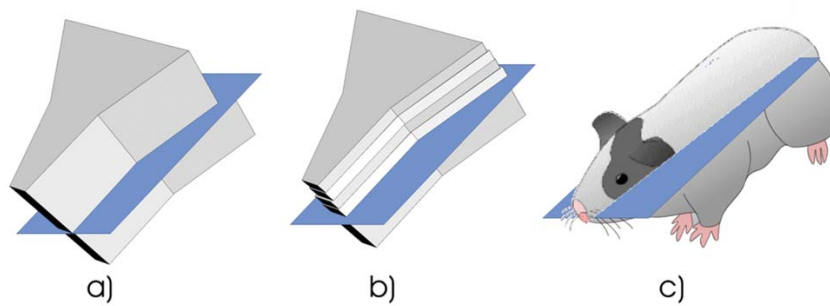


Figure 17. Schematic drawing of phantoms (a and b) and frozen animal (c) used for comparison of dosimetry. Phantoms and frozen animal were irradiated with radiochromic films placed at the cochlear plane.

Irradiation fields

Three collimators with different irradiation fields from 5 mm thick lead sheets 15 cm x 30 cm in size were constructed. Irradiation field sizes (12 mm diameter, 5.7 mm diameter and a 6.5 x 7.2 mm respectively) were placed at 10 cm from the anterior border of the collimator in the midline. The lead shield covered the entire animal leaving the window for the right or left cochleae depending on the chosen irradiation side. For our purposes, the irradiation fields were centered over the left cochlea in all the experiments.

Frozen animal landmarks and confirmatory CT scan

For frozen animal irradiations, the external ear canal was used as landmark to locate the cochlea on the anterior-posterior axis, whereas a mark 4 mm from the midline at

the cranial skin surface was used to locate the area of the left cochleae. With the final irradiation field, a second confirmatory CT scan was performed using these landmarks. The lead collimator was changed for a PVC slab with a hole of 6.5 x 7.2 mm and placed over the left cochlea (Figure 16d).

Irradiation system and parameters

For irradiation purposes, the restrainer was positioned inside the Faxitron CP-160 Cabinet X-Radiator System (Faxitron X-Ray Corp., Wheeling, IL, USA) on tray guide #8 (source to surface distance of 22.9 cm). Added filtration used was a 0.5 mm Cu filter and the beam parameters were set at maximum (160 kVp at 6.3 mA). All the films were placed at the cochlear plane and irradiations conducted at a programmed exposure time of 1.2 minutes. The surface to source distance in the animal and phantoms was maintained homogenously for a total of 17.3 cm throughout all the experiments.

Radiochromic film dosimetry

EBT Radiochromic films (International Specialty Products, Wayne, NJ) were cut to a size of 3" × 5" in order to fit the size of the phantom in the restrainer. The spatial dosimetry was performed using an Epson Expression 10000XL flatbed document scanner (Epson, Nagano, Japan). For each irradiation field (12 mm diameter, 5.7 mm diameter and 6.5 x 7.2 mm) and phantoms, five film pieces were scanned prior to, and 24 h following irradiation with EPSON SCAN 3.01A software, with maximum optical density (OD) range. In addition, all filters and image enhancement options were turned off. The films were scanned in the 48-bit RGB mode (16 bits per color) and saved as tagged image file format (TIFF) image files. All images were scanned with an image resolution of 127 dpi, which translates into 0.2 mm/pixel. Accordingly, the 2 × 2 mm² regions of interest over which the *netODs* were determined consisted of 10 × 10 pixels. To quantify the change in optical density due to the irradiation only, a control film was used. This film piece had the same size and initial optical density and was carried over the experiment without being irradiated.

The radiochromic films were handled in accordance with the recommendations outlined in the AAPM TG-55 report ⁽¹⁵²⁾. The change in the OD of the control films was subtracted from the exposed films to obtain the final *netOD* that was converted to dose using the formalism described by Devic et al. ⁽¹⁵³⁾. Furthermore, measured change in optical density from the films was averaged and converted into dose using previously established calibration curve. Calibration curve was constructed by irradiating film pieces to known doses within a reference beam of the same quality and output specified following the AAPM TG-61 protocol ⁽¹⁵⁴⁾. With the curve and the irradiated films, estimates of doses received at different distances from the center of the beam were calculated in Grays (Gy).

Results

Collimator sizes

Given that the endpoint for this model is cochlear damage, the size of the irradiation field was decided to cover not only the cochlea per se but also to give a margin of dose deposition error of at least 2 mm. The actual irradiation field detected by the radiochromic film at the cochlear plane was larger than collimator size, which is a result of the divergent nature of the beam used. Comparisons of doses using different collimator sizes in phantom 1 are shown in Table 3. A 12 mm diameter irradiation field was capable of irradiating completely the midline and partially the temporal bone of the contra lateral side; whereas a 5.7 mm diameter irradiation field was too small leaving a very narrow margin of error (<1 mm). The spatial distribution was evaluated and a final collimator size of 6.5 x 7.2 mm for the dosimetry measurements in different phantoms was determined to be used. With the collimator chosen, the margins received 50% of the total dose, allowing proper unilateral irradiation without irradiating the midline or the contra-lateral ear at complete doses. This was corroborated with a confirmatory CT scan using a PVC slab with a hole of an equal size as the collimator (Figure 16d).

TABLE 3. *Comparison of dose deposition between collimator sizes.*

Collimator size (mm)	Irradiation field size (mm)	Midline Dose (%)	Non-irradiated cochlea dose (%)
12 diam.	14.8 diam	96%	6.6%
5.7 diam.	6.7 diam.	8.6%	1.5%
6.5 x 7.2	7.8 x 8.6	57%	1.94%

Table 3. The final collimator size (6.5 x 7.2) provided an irradiation field with a margin of 2 mm while the marks representing the midline structure and the opposite cochlea received 57 % and 1.94 % of the total dose respectively. mm = millimetres. diam= diameter.

The variation of dose at the entire central region of the radiated field was 4% in both phantom 1 and 2. Phantom 1 (PVC) was used only to define the collimator size, revealing a dose rate of 1.80 Gy/minute at the cochlear plane as shown in Table 4. Using phantom 2 with tissue substitute materials a dose rate of 1.55 Gy/minute was obtained, suggesting that a large dose variation can be expected due to tissue inhomogeneities (bone, air). Therefore it was decided to perform a more realistic dose measurement using the frozen animal. In phantoms, the dose rate measured at the contra-lateral cochlea (8 mm) was determined 1.94 – 3.2% of the central dose delivered. As for the midline structures, the brainstem (4 mm) received 45 to 57% of the dose applied to the cochlea. Nevertheless, when performing dosimetry in the frozen guinea pig, an asymmetric output was obtained. A proposed solution to obtain a dose rate was to measure the outputs at the medial, center and lateral portions of the irradiation field, then average the dose rates. Using this method, a final dose rate of 1.35 Gy/min was obtained in the real tissue (Figure 18).

TABLE 4. *Comparison of dose deposition between phantoms and real tissue.*

	Material	Dose rate (Gy/min)	Midline (Gy)	Total dose (%)	Non irradiated cochlea (Gy)	Total dose (%)
Phantom 1	PVC	1.80 ± 0.04	1.03 ± 0.33	57%	0.035±0.01	1.94%
Phantom 2	PVC+teflon	1.55 ± 0.02	0.69 ± 0.14	44.5%	0.05±0.01	3.22%
Frozen GP	Real tissue	1.2-1.5 ± 0.02 (1.35 Av)	0.13 ± 0.04	9.85%	0.035±0.01	2.59%

Table 4. The dose rate obtained at the center of the beam positioned over the left cochlea was less in the frozen guinea pig. The left cochlea and the midline structures receive less radiation in the real tissue, demonstrating the overestimating effect of radiation dosimetry in phantom animals. GP = guinea pig ; PVC = polyvinyl chloride; Gy = Gray; min = minute; Av = average. Values are means \pm standard deviation.

Discussion

The final irradiation field of 6.5 x 7.2 mm was preferred over bigger sizes to avoid mortality and acute morbidity when using radiation on guinea pigs (i.e. ear canal stenosis and otitis media with effusion). These complications can affect the proper recording of functional measurements due to ineffective sound propagation waves through air conduction. In addition, the auditory pathway fibers decussate at the level of the brainstem, thus, it is very important to keep irradiation to this area as low as possible even though it represents a resilient tissue⁽⁴²⁾.

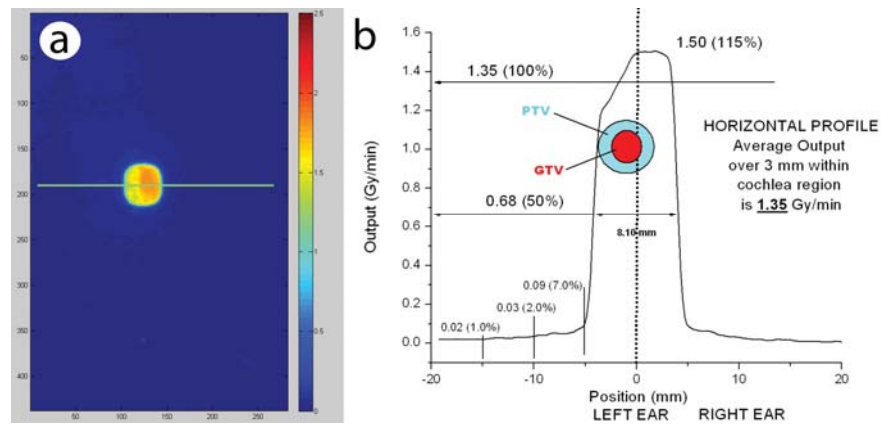


Figure 18. Dosimetry in the frozen animal. At the horizontal profile of the irradiation field, dosimetry revealed asymmetric dose absorption at the cochlear plane. PTV = planned target volume; GTV = gross target volume.

Our findings emphasize the need of preliminary dosimetry in real tissue when irradiating the cochleae. As seen in our system when using kV the dose deposition was highly dependent on bone tissue. This explains the asymmetry in dose absorbed at the radiochromic film in the frozen animal when compared with tissue substitute materials.

The differences in dosimetry found between the phantoms and the frozen animal further explain the variation in outcomes of studies involving sensorineural hearing

loss after radiotherapy (Table 5). Only a few animal studies in radiation-induced sensorineural hearing loss have taken into consideration the radiation doses delivered at the cochlear plane. Winther ⁽¹⁰⁷⁾ used a press-wood phantom guinea pig head to obtain the output of his irradiation system. Using such method, he observed that the non-irradiated ear received 4% of the total dose, while Gamble ⁽¹⁵⁵⁾ using a different collimator size, reported that 8% of the total dose was delivered. Nagel and Schafer ⁽¹⁵⁶⁾ using a ionization chamber reported that 2.7% of the total dose reached the non-aimed ear. These studies underline the importance of the identification of non-irradiated ear doses; however the most important challenge remains determining the exact dose actually delivered to the irradiated cochlea. As seen in our findings, the previously mentioned was most undoubtedly not overcome by the single material phantom method. Therefore, the outcomes of hearing loss in single-dose radiation studies could be explained by the large doses applied to the cochlea more than precise doses.

Thermoluminescent dosimeters have also been used in live animals by placing them in the skin surface proximal to a transversal beam directed to both cochleae ⁽¹⁵⁷⁾. Nonetheless this method, which is also sensitive to light and temperature of the animal skin, did not take into account the variability of the bone tissue. The use of TLDs on skin surfaces to estimate delivered dose at deep regions with tissue inhomogeneities precludes giving an accurate dose rate at the cochlear depth, thus the radiation dose delivered was approximated and not precisely controlled.

Apart from these early reports, the rest of the literature on radiation-induced cochlear damage fails to report a detailed dosimetry method at the cochlear depth ^(41, 108, 109, 116, 118, 145, 158). As we demonstrated in this work, the use of tissue substitute materials or surface methods can overestimate machine's dose deposition at the cochlear level. For example, the study by Greene et al. ⁽¹⁴⁵⁾, which intended to use fractionated RT with 2 Gy fractions, found no cochlear damage after a total dose of 70 Gy one year after treatment. However, their findings could be the result of an inappropriate method of dosimetry and therefore a lower dose delivered on each fraction and subsequently in total dose. As shown in this present study the use of dosimetry in a single material

phantom could have overestimated the dose rate by 25% when compared to the real tissue. Thus, in terms of external validity the reporting of dosimetry method and the cochlear dose rate in real tissue should be examined in future studies involving animal models.

The method presented in this work allowed us to refine the irradiation field size while minimizing dose delivery to adjacent structures. Moreover, it permitted to obtain an accurate dose rate for our irradiation system ultimately assuring a reproducible and reliable small-animal irradiation setup. In our radiation system, a 2 Gy dose to the cochlea would require 1.5 minutes of exposure, while the contra-lateral ear would receive 0.05 Gy. In the case of single-dose irradiations (i.e. 60 Gy) using the setup described in this study, the animals would receive 2.59 % of the total dose at the non-irradiated ear, which is considered negligible and is not expected to cause cochlear damage. The brainstem would receive almost 10% of the total dose which in clinical doses would be below the reported permissive dose to this area ⁽¹⁵⁹⁾. Thus, the setup of the present study could be used with confidence bearing in mind that the non-irradiated cochleae could be used as control and that the brainstem receives negligible radiation doses.

Considering that the target volume is small, a large error in the target localization and the dose delivered to the cochlea could be introduced. This fact points out a weakness in our setup. However, given that the main endpoint is hearing loss, this last flaw could be overcome by increasing the irradiation field with a potential exchange of irradiation to adjacent structures. Therefore, it was decided to leave a margin of at least 2 mm of the radiation field. A limitation of the dosimetry method presented is the inability to measure the heterogeneity at the entire volume of the cochlea. Nevertheless, this problem most probably will be encountered in all other methods intended for dosimetry given the complexity of the inner ear anatomy.

Despite these limitations, the proposed method allowed adjustment of the collimator size and dose rate calculation, which can be of benefit in other studies

TABLE 5. *Parameters and methods of dosimetry reported in the literature using the guinea pig model of cochlear irradiation.*

Author and year	Scheme (Total Dose)	Energy	Orientation and size (mm)	Dosimetry method	Dose at Non- irradiated ear	Outcome
Winther 1968 ⁽¹⁰⁷⁾	Single (10-70 Gy)	290 kV (12 mA)	Unilateral 20 x 17	Ionization chamber in press wood phantom	4%	Damage after 40 Gy
Gamble 1968 ⁽¹⁵⁵⁾	Single (5-60 Gy)	250 kV	Unilateral 10 diam.	Estimated	8.3%	Damage after 30 Gy
Nagel 1984 ⁽¹⁵⁶⁾	Single (35-70 Gy)	290 kV (12 mA)	Unilateral 17 x 11	Ionization chamber in phantom	2.7%	Damage after 40 Gy
Tokimoto 1985 ⁽¹⁰⁹⁾	Single (20-120 Gy)	200 kV (20 mA)	Unilateral 15 x 15 or 20 x 30	NR	NR	Damage after 80 Gy
Ohashi 1988 ⁽¹⁵⁸⁾	Single (30 Gy)	200 Kv	Bilateral 40 x 20	NR	NR	Deterioration of ciliary activity (middle ear)
Greene 1992 ⁽¹⁴⁵⁾	Fractionated 7 weeks (57.5-70 Gy)	200 kV (20 mA)	Unilateral	NR	NR	No damage
Kim 1994 ⁽¹⁰⁸⁾	Single (2-15 Gy)	24 MeV Neutron	Unilateral	NR	NR	Damage after 10 Gy - 15 Gy.
Miller 2009 ⁽¹⁵⁷⁾	Fractionated 5 weeks (61 RE, 70 LE)	250 kV	Transversal beam	Mastoid surface TLD	(87%-RE, 100% LE)	More damage with RT and cisplatin
Altas 2006 ⁽¹¹⁸⁾	Fractionated 1 week (33 Gy)	Cobalt 60 MV	Total cranial	Estimated	NA	L-Carnitine ameliorates radiation induced damage
Altas 2006 ⁽⁴¹⁾	Fractionated 1 week (33 Gy)	Cobalt 60 MV	Total cranial	Estimated	NA	Piracetam ameliorates radiation induced damage
Lessa 2009 ⁽¹¹⁶⁾	Single (350 cGy)	Cobalt 60 MV	Bilateral	NR	NR	Cytoprotection of amifostine

The guinea pig has been used as model for cochlear irradiation; however there is a high heterogeneity in the schemes, dosimetry methods and irradiation fields. Most of the studies fail in the reporting of doses to the irradiated and non-irradiated cochleae and the description of dosimetry methods. Gy = grays; cGy = centigrays; RE = right ear; LE = left ear; kV = Kilovoltage; MeV = megaelectron volt; MV = Megavoltage; diam = diameter; NR = not reported; NA = not applicable. mA = milliampere; RT = radiotherapy.

involving organs surrounded by bony structures such as the head and neck. In addition, the radiochromic films can be also used as a dose monitoring tool, by placing pieces of film beneath the animal. While the actual dose value derived from the film's *netOD* of the monitoring film piece is of no importance, variation between different film pieces (corresponding to different irradiations) can be used to monitor the actual dose delivered in every single experiment.

Conclusion

The proposed method allowed better specification of the irradiation field in an animal model of cochlear irradiation. Using irradiation systems of kilovoltage range energies, the dose absorption at the cochlear plane in the guinea pig was asymmetric, which is not the case for phantoms. Thus, reporting of dosimetry at the cochlear level in real tissue should be encouraged in future studies involving cochlear irradiation.

Chapter 3.3. In vivo evaluation of radio-protective effects of Metformin in the guinea pig cochlea.

Introduction

The next set of experiments will use the results of the preliminary *in vivo* experiments (described in Chapter 3.2) to deliver known radiation doses to the guinea pig cochlea.

Objective

To evaluate whether Metformin is radio-protective to the guinea pig cochlea in a scheme of fractionated radiotherapy.

Methods

Protocol

One week before radiation exposure started, 15 animals received baseline audiometric testing. Three days before this exposure, 8 animals started receiving Metformin in their water while the remaining 7 received normal drinking water. Then, all animals received unilateral radiation on 20 consecutive days, with the side of radiation being randomly chosen. One week and 6 weeks after completion of radiation, all animals again received audiometric testing. Details are described below.

Animal subjects

Fifteen six-week-old female albino guinea pigs (450 to 500 g) were purchased from Charles River Laboratories (Wilmington, Massachusetts, U.S.A). Only animals with normal ear anatomy and hearing were used. The animals had free access to food and water. Animals were kept in standard housing at $22 \pm 4^{\circ}\text{C}$ ambient temperature with a relative humidity of $50 \pm 5\%$ and a 12-hour light/dark cycle until the animals with Metformin on drinking water were separated in individual cages. The animals were kept in the animal care research facilities of The Montreal Children's Hospital Research Institute. The animals were monitored daily for signs of pain, weight loss or head tilt.

Experimental set-up

The animals were divided in two groups depending on whether they received drinking water with Metformin or regular water. One ear of each animal was randomly (by tossing a coin) chosen for radiation. This resulted in four testing groups: control (water, no radiation, n=7), irradiated (water, radiation, n=7), Metformin (Metformin, no radiation, n=8) and experimental (Metformin, radiation, n=8). The radiation side could always be identified, initially, by marking the fur over the radiation field, and later, by a region of fur loss over the irradiation field which appeared in every animal. The study was approved by the McGill University Animal Care Committee.

Animal restrainer

A restrainer from the original design described by Winther ⁽¹⁰⁷⁾ was constructed. The device allowed a protective lead shield to be used under a radiation source. The front teeth of the guinea pig serve to suspend the head from a horizontal 1 mm diameter wire while two opposing lateral screws keep the animal's head immobile. The collimator with a hole for the irradiation field was supported by the walls of the restrainer and placed on above the animal, covering the entire body with the exception of the region to be irradiated.

Irradiation system

The animals were anesthetized under inhalational anesthesia, restrained and placed in the restrainer. The side to receive radiation could be easily identified (see above). Once anesthetized, the animal in the restrainer was positioned inside the Faxitron CP-160 Cabinet X-Radiator System (Faxitron X-Ray Corp., Wheeling, IL, USA) on tray guide #8 (source to surface distance of 22.9 cm). Added filtration used was a 0.5 mm Cu filter and the beam parameters were set at maximum (160 kVp at 6.3 mA). All the irradiations were conducted at a programmed exposure time of 2.6 minutes. The fraction size was 3.5 Gy per day given from Monday to Friday for four weeks totaling a dose of 71 Gy.

A collimator was constructed from 5 mm thick lead sheets with a size of 15 cm x 30 cm. An irradiation field size of 6.5 x 7.2 mm was placed at 10 cm from the anterior

border of the collimator at the midline level. The lead shield covered the entire animal leaving the window for the the chosen irradiation side. Having the the lead sheet in position and using external landmarks (external ear canal and 4 mm from the midline), the beam center of the x-ray tube was positioned over the unshielded ear to be irradiated. The animals were kept under inhalational anesthesia through a mask connected to the anesthetic vaporizer during the complete delivery of each fraction.

Dosimetry calculation

The dosimetry calculation was performed as described in the previous chapter with EBT Radiochromic films. The output of 1.35 Gy obtained in the experiments was used to calculate the exposure time in the irradiation system.

Metformin administration

Metformin (LKT Laboratories, St Paul, MN, USA) was administered in the drinking water of the animals three days before the starting of the radiation therapy and until the end of the experiment. Given that guinea pigs drink on average 10 to 15 ml/100g of body weight /day ⁽¹⁶⁰⁾ and no change in daily water intake was reported on previous studies ⁽¹³⁶⁾, Metformin was dissolved in the drinking water to give a dose of 100 mg/kg. Studies have not reported toxicity at at this dose, either intraperitoneally or orally⁽¹⁶¹⁾. The drinking bottles were prepared with a solution of Metformin and changed biweekly according to body weight changes to have dose consistency.

Assessment of ototoxicity: Auditory Brainstem Response

The auditory testing was performed under general anesthesia with inhaled isoflurane. The tympanic membranes and external auditory canals were inspected before the functional evaluation. ABR testing was performed prior to any treatment (baseline measurement) and 1 week and 6 weeks following the end of radiotherapy treatment to determine the hearing threshold shifts. The last time point was chosen because this is the usual time course for the acute effects of RT to subside according to previous studies ⁽¹⁵⁷⁾. Since it was expected that animals would develop middle ear effusion and to avoid improper functional testing, a 2 mm incision in the tympanic membrane of each ear was performed before every functional measurement in order to prevent

effusion accumulation in the tympanic bulla. A surgical aspirator was used if required to drain effusions. This was consistently performed to decrease artifacts during the functional measurements of the experiment and to decrease complications from radiation treatment. Bilateral ABR testing was performed using the SmartEP System (Intelligent Hearing Systems, Miami FL). Responses were recorded from stainless steel needle electrodes placed subdermally at the pinna of the ear tested (active), vertex (reference), and contralateral pinna (ground). Tone burst stimuli (8, 16, 20, and 25 kHz) with Blackman envelope were presented at a rate of 39.1 bursts per second through insert earphones. The stimuli were presented at 80 dB sound pressure level, decreasing in steps of 20, 10, and 5 dB to estimate the threshold. Responses to the stimuli were amplified, filtered, and averaged over 1,600 sweeps. The ABR threshold was defined as the lowest intensity where three reproducible waves could be obtained. Threshold shifts were calculated by comparing the hearing threshold values between the different time points and the baseline.

DPOAE measurements

Measurements were obtained using the SmartDPOAE system (Intelligent Hearing System, Miami, FL). The f2/f1 ratio was 1.2, and the intensity of the stimulus was 65 dB. The frequency of f2 varied between 0.8 and 35 kHz for a total of 18 different recording points. Prior to each DPOAE recording, the seal and position of the ear probe was verified by monitoring the amplitude of calibration signals within the ear canal. Each point was recorded twice, and the average was used for analysis. Baseline and post-treatment DPOAE measurements were obtained under anesthesia to monitor a change in hearing, according to the protocol previously described.

Statistical analysis

The mean change between every measurement and baseline ABR and DPOAE at each frequency was calculated. Differences between the 4 groups were evaluated with the non-parametric Kruskal-Wallis test. The Dunn's post-hoc test was subsequently performed for further analysis between pairs of groups. Statistical significance was set at $p \leq 0.05$. Results are presented as mean \pm standard error of the mean (SEM).

Statistical analysis was completed using GraphPad Prism Software Inc (La Jolla,CA,USA).

Results

Threshold shifts in ABR measurements between baseline and post-radiotherapy treatment were compared at four frequencies between different groups at week one and at week six. At week one (Figure 19), there was a suggestion that the Metformin was having a protective effect in the experimental group (Metformin + radiation) when compared to the irradiation group, however, no statistically significant differences were found when all four frequencies were considered.

At one week after the completion of radiotherapy, 3 ears in the group of radiotherapy and 3 more in the experimental had middle ear effusions as confirmed by otoscopy. However, this was resolved with tympanotomy, as was corroborated at the week 6 hearing evaluation where otoscopy confirmed no residual effusion.

Six weeks after the completion of radiotherapy (Figure 20), there was increased hearing loss in both groups receiving RT, with animals in the experimental group exhibiting less hearing loss. However, the differences were still not statistically significant between the groups at this second time point. The only statistically significant differences found were at two frequencies between the Metformin only and the radiotherapy only groups ($p < 0.05$), but this likely has little clinical importance.

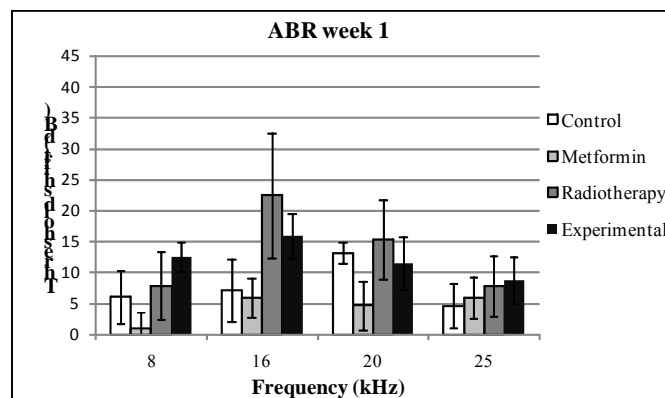


Figure 19. Mean ABR threshold shift per frequency one week after completion of radiotherapy in control (n=7), Metformin (n=8), radiotherapy (n=7) and experimental ears (n=8). The data represent mean \pm standard deviation.

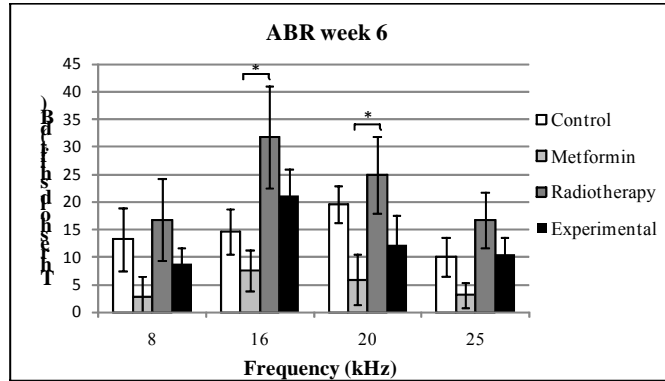


Figure 20. Mean ABR threshold shift per frequency six week after completion of radiotherapy in control (n=7), Metformin (n=8), radiotherapy (n=7) and experimental ears (n=8). The data represent mean \pm standard deviation.

When results associated with DPOAE measurements were examined, there was a slight decrease in DPOAE amplitude in all groups between the baseline and the time points after completion of radiotherapy. Baseline measurements did not show any differences between groups for the eighteen frequencies tested (Figure 21). One week after completion of radiotherapy, DPOAE amplitudes at only two frequencies in the range of 13.2 and 17.6 kHz exhibited statistically significant differences (Figure 22). These were between the Metformin only and radiotherapy only, groups ($p < 0.05$). At week six, the same groups showed differences at only one frequency (6.6 kHz, $p < 0.05$) (Figure 23).

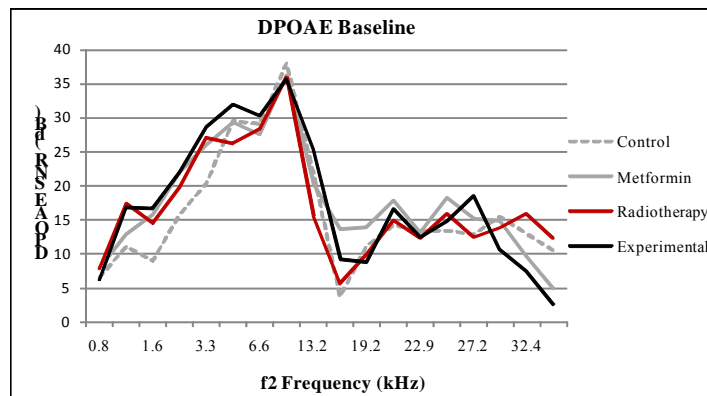


Figure 21. Mean DPOAE signal to noise ratio per frequency at baseline in control (n=7), Metformin (n=8), radiotherapy (n=7) and experimental ears (n=8).

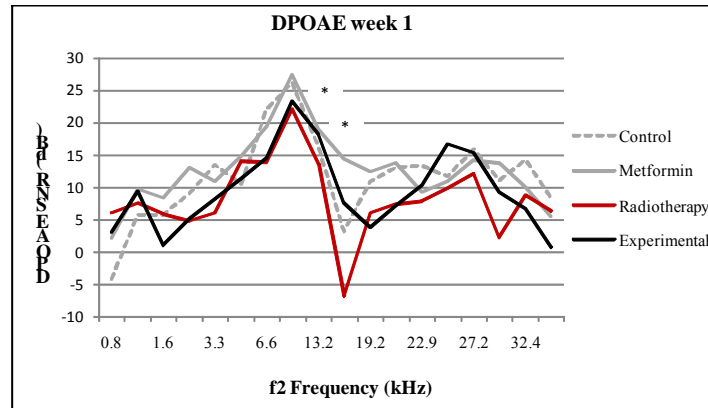


Figure 22. Mean DPOAE signal to noise ratio per frequency after one week of completion of radiotherapy in control (n=7), Metformin (n=8), radiotherapy (n=7) and experimental ears (n=8).

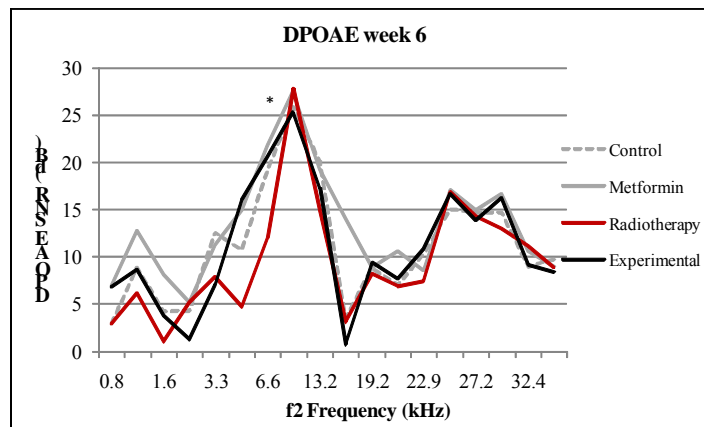


Figure 23. Mean DPOAE signal to noise ratio per frequency after six weeks of completion of radiotherapy in control (n=7), Metformin (n=8), radiotherapy (n=7) and experimental ears (n=8).

Discussion

Unfortunately, appropriate methodological description is missing in the literature describing animal models of cochlear irradiation and was the main challenge found in setting up the animal experiments. As evidence of this, studies without dosimetry have reported better hearing outcomes in animals subjected to radiotherapy⁽¹⁴⁵⁾. A study using surface dosimetry with TLD's have reported that animals had a hearing loss of almost 50 dB over the different frequencies tested (0-15 kHz) six weeks after completion of a radiation (smaller fraction size and a total dose of 71 Gy)⁽¹⁵⁷⁾. Therefore, the corroboration of doses using radiochromic films is of vital importance for our study in terms of external validity, reproducibility and future projects.

Despite the decrease in DPOAE testing over time, analysis showed that there were no differences between the experimental and radiotherapy groups at the different time points evaluated. These results suggest that radiation or Metformin treatment did not have any effect at the level of the outer hair cells. Nevertheless, it is surprising that at week-one and at week-six post-radiotherapy, two and one frequencies, respectively, demonstrated that in the Metformin group, the ears had larger DPOAE amplitudes than the radiated ears – results similar to that seen in ABR testing. Again, this is unlikely to have clinical significance.

One week after radiotherapy, ABR testing showed, at 2 testing frequencies, the expected increase in hearing threshold, but this increase was not statistically significant. Six weeks after radiotherapy, the expected increase in hearing threshold was seen at all 4 frequencies. However, again the differences in threshold shifts were not statistically significant. These results could be explained by the fact that Metformin is not otoprotective, or by the fact that the degree of radiation damage was still not enough to produce a significant effect. Given that RISNHL requires a prolonged time to develop, the radio-protective effects of Metformin might become more evident in a study having a longer follow-up. Another possible explanation of these findings is that Metformin levels might have not been high enough in the guinea pig inner ear to be effective. It is unknown whether Metformin crosses the blood-brain barrier in guinea pig at the same rate that it does in other previously tested species⁽¹²⁶⁾.

Interestingly, the ears subjected only to Metformin showed better ABR thresholds and larger DPOAE response amplitudes in some frequencies compared to the rest of the groups. These apparently beneficial effects might be corroborated in further studies assessing the antiaging effects of Metformin⁽¹⁶²⁾ in the auditory system.

It is interesting that possible radiation effects on DPOAE measurements were less than possible radiation effects on ABR measurements. If this trend were confirmed in subsequent longer studies, this would support the idea of a predominant neural component in radiation-induced damage in fractionated radiotherapy involving - most probably the inner hair cells or the spiral ganglia neurons⁽¹¹⁰⁾. This would suggest that

there might be a differential damage to structures in the cochlea, which might explain the minimal differences found in DPOAE amplitudes between the four groups.

In terms of middle ear effusion, 3 animals in each group had effusion, which were adequately managed by incision of the tympanic membrane and aspiration. As seen with the DPOAE's where there were no differences between irradiated and control ears, it is unlikely that middle ear effusion could have affected our measurements in this animal model.

The limitations of the current study include the small sample size used for the *in vivo* experiments, which might not have had enough statistical power to detect differences between experimental and radiotherapy groups. A second limitation follows because RISNHL is a late and progressive adverse effect, suggesting that the follow-up in this study could have been too short to detect differences between groups. Thirdly, a dose response evaluation of Metformin is also needed in order to corroborate the hypothetical effects of this drug in the auditory pathway. Unfortunately in this study, a histological evaluation of hearing was not performed, nor was another analytical tool, such as PCR or western blot analysis, which might have determined whether Metformin decreased the production of reactive oxygen species or cell death markers in the cochlea.

Future directions of this study would include: (a) a longer-term follow-up of at least 16 weeks after radiotherapy treatment, (b) evaluation of the sample size required with enough power to detect differences after 16 weeks and also, (c) performance of a dose response effect of Metformin in case significant differences are found between the groups. In addition, it would be useful to extend the analysis to other tissues which were subjected to irradiation, such as brain or skin. This could help to corroborate if Metformin might serve as a radioprotective agent in fractionated radiotherapy.

Conclusion

Metformin was ineffective as radio-protective agent in the guinea pig cochlea.

PART FOUR: Overall Conclusion

Chapter 4.1. Conclusion

The systematic review performed in this thesis demonstrated that RISNHL is a late, progressive and dose-dependent effect after fractionated therapy for head and neck cancer.

Currently there is only one compound with proven radioprotection effect (on the salivary glands), demonstrating the need for more research on preclinical models of radiotherapy and radioprotective agents. Therefore, this project aimed to determine the safety and radioprotective properties of Metformin, a compound which has been shown to have anticancer and antioxidant properties.

A guinea pig model of radiation-induced sensorineural hearing loss was refined, revealing asymmetrical cochlear dose absorption, which can result in dose overestimation if proper dosimetry is not performed as was seen to be common in most of the previous literature.

Experiments *in vivo* and *in vitro* demonstrated that Metformin is not ototoxic. The ears of animals given Metformin in drinking water and subjected to radiotherapy showed a non-statistically significant decrease of hearing loss when compared to the radiated ears at six weeks post-radiation while ears subjected solely to Metformin had better hearing thresholds. The findings of this study corroborate Metformin's safety in the auditory system. Given the characteristics of RISNHL, the short follow-up period between irradiation and hearing tests performed in this study, prevents making definitive conclusions about Metformin's possible role as a radioprotector. This question remains to be answered in a study having with a larger sample size, over a longer follow-up period, perhaps including a dose-dependency investigation.

The refined animal model and the now-demonstrated safety of Metformin provide a firm platform for further research in radiation-induced cochlear damage and ototoxicity prevention studies.

References

1. Canadian Society of Otolaryngology Head and Neck Surgery. Elora: Canadian Society of Otolaryngology Head and Neck Surgery; [cited 2011 November 28th]; Available from: <http://www.entcanada.org/public2/patient14.asp>.
2. Fleury B, Lapeyre M. [Tolerance of normal tissues to radiation therapy: ear]. *Cancer Radiotherapie*. 2010;14(4-5):284-9. Dose de tolerance a l'irradiation des tissus sains: l'oreille.
3. Raaijmakers E, Engelen AM. Is sensorineural hearing loss a possible side effect of nasopharyngeal and parotid irradiation? A systematic review of the literature. *Radiotherapy and Oncology*. 2002;65(1):1-7.
4. van der Putten L, de Bree R, Plukker JT, Langendijk JA, Smits C, Burlage FR, et al. Permanent unilateral hearing loss after radiotherapy for parotid gland tumors. *Head and Neck*. 2006;28(10):902-8.
5. Ondrey FG, Greig JR, Herscher L. Radiation dose to otologic structures during head and neck cancer radiation therapy. *The Laryngoscope*. 2000;110(2 Pt 1):217-21.
6. Low WK, Tan MG, Chua AW, Sun L, Wang DY. 12th Yahya Cohen Memorial Lecture: The cellular and molecular basis of radiation-induced sensori-neural hearing loss. *Annals of the Academy of Medicine, Singapore*. 2009;38(1):91-4.
7. Lyng FM, Seymour CB, Mothersill C. Oxidative stress in cells exposed to low levels of ionizing radiation. *Biochemical Society Transactions*. 2001;29(Pt 2):350-3.
8. Leach JK, Van Tuyle G, Lin PS, Schmidt-Ullrich R, Mikkelsen RB. Ionizing radiation-induced, mitochondria-dependent generation of reactive oxygen/nitrogen. *Cancer Research*. 2001;61(10):3894-901.
9. Ben Sahra I, Le Marchand-Brustel Y, Tanti JF, Bost F. Metformin in cancer therapy: a new perspective for an old antidiabetic drug? *Molecular Cancer Therapeutics*. 2010;9(5):1092-9.
10. Sikka A, Kaur M, Agarwal C, Deep G, Agarwal R. Metformin suppresses growth of human head and neck squamous cell carcinoma via global inhibition of protein translation. *Cell Cycle*. 2012;11(7):1374-82.
11. Guigas B, Demaille D, Chauvin C, Batandier C, De Oliveira F, Fontaine E, et al. Metformin inhibits mitochondrial permeability transition and cell death: a pharmacological in vitro study. *Biochemical Journal*. 2004;382(Pt 3):877-84.
12. El-Mir MY, Demaille D, G RV, Delgado-Esteban M, Guigas B, Attia S, et al. Neuroprotective role of antidiabetic drug Metformin against apoptotic cell death in primary cortical neurons. *Journal of molecular neuroscience : MN*. 2008;34(1):77-87.

13. Morales AI, Demaille D, Prieto M, Puente A, Briones E, Arevalo M, et al. Metformin prevents experimental gentamicin-induced nephropathy by a mitochondria-dependent pathway. *Kidney International*. 2010;77(10):861-9.
14. Chang J, Jung HH, Yang JY, Choi J, Im GJ, Chae SW. Protective role of antidiabetic drug Metformin against gentamicin induced apoptosis in auditory cell line. *Hearing Research*. 2011;282(1-2):92-6.
15. Salvi R, Sun W, Lobarinas E. Anatomy and Physiology of the Peripheral Auditory System. In: Roeser R, Valente M, Hosford-Dunn H, editors. *Audiology Diagnosis*. 2nd Edition ed. New York: Thieme; 2007. p. 17-36.
16. Ream TD. Removal of Cerumen and Foreign Bodies from the Ear. In: R. D, D.P. A, editors. *Essential Clinical Procedures*. 2nd ed. Philadelphia: Elsevier Saunders; 2007. p. 445-52.
17. Raphael Y, Altschuler RA. Structure and innervation of the cochlea. *Brain Research Bulletin*. 2003;60(5-6):397-422.
18. Lim DJ. Chapter 24. Ultrastructural Anatomy of the Cochlea. In: Van-De-Water TR, Staeker H, editors. *Otolaryngology Basic Science and Clinical Review* New York: Thieme; 2006. p. 313-31.
19. Gillespie PG. Chapter 25. Hair Cell Function. In: Van-De-Water TR, Staeker H, editors. *Otolaryngology: Basic Science and Clinical Review*. New-York: Thieme; 2006. p. 332-9.
20. Bosher SK, Warren RL. Observations on the electrochemistry of the cochlear endolymph of the rat: a quantitative study of its electrical potential and ionic composition as determined by means of flame spectrophotometry. *Proceedings of the Royal Society of London Series B: Biological Sciences*. 1968;171(23):227-47.
21. Hudspeth AJ. Hair-bundle mechanics and a model for mechanoelectrical transduction by hair cells. *Society of General Physiologists Series*. 1992;47:357-70.
22. Musiek FE, Weihing JA, Oxholm VB. Anatomy and physiology of the Central Auditory Nervous System: A Clinical Perspective. In: Roeser R, Valente M, Hosford-Dunn H, editors. *Audiology Diagnosis*. New-York: Thieme; 2007. p. 37-64.
23. Dublin WB. The cochlear nuclei--pathology. *Otolaryngology - Head and Neck Surgery*. 1985;93(4):448-63.
24. Goldberg JM, Moore RY. Ascending projections of the lateral lemniscus in the cat and the monkey. *Journal of Comparative Neurology*. 1967(129):143-55.
25. Aitkin LM, Webster WR, Veale JL, Crosby DC. Inferior colliculus. I. Comparison of response properties of neurons in central, pericentral, and external nuclei of adult cat. *Journal of Neurophysiology*. 1975;38(5):1196-207.

26. Musiek FE, Baran JA. Neuroanatomy, neurophysiology, and central auditory assessment. Part I: Brain stem. *Ear and Hearing*. 1986;7(4):207-19.
27. Noback CR. Neuroanatomical correlates of central auditory function. In: M.L. P, F.E. M, editors. *Assessment of central auditory dysfunction: Foundations and clinical correlates*. Baltimore: Williams & Wilkins; 1985. p. 7-21.
28. Middlebrooks JC. Auditory System: Central Pathways. In: Squire L, editor. *Encyclopedia of Neuroscience*: Academic Press; 2009. p. 745-52.
29. French JD. The reticular formation; the nature of the reticular activating system. *Journal of Neurosurgery*. 1958;15(1):97-115.
30. Hall EJ, Cox JD. Physical and Biologic Basis of Radiation Therapy. In: Cox JD, Ang KK, editors. *Radiation Oncology Rationale Techniques Results 9th edition*. ed: Mosby Elsevier; 2010. p. 3-49.
31. Sharma RA, Vallis KA, McKenna WG. Chapter 29. Basics of Radiation Therapy. In: Abeloff MD, editor. *Abeloff's Clinical Oncology*. 4th ed. Philadelphia: Churchill Livingstone; 2008.
32. Thwaites DI, Tuohy JB. Back to the future: the history and development of the clinical linear accelerator. *Physics in Medicine and Biology*. 2006;51(13):R343-62.
33. Ogawa Y, Kobayashi T, Nishioka A, Kariya S, Hamasato S, Seguchi H, et al. Radiation-induced reactive oxygen species formation prior to oxidative DNA damage in human peripheral T cells. *International Journal of Molecular Medicine*. 2003;11(2):149-52.
34. Ward JF. Biochemistry of DNA lesions. *Radiation Research Supplement*. 1985;8:S103-11.
35. Buatti JM, Friedman WA, Meeks SL, Bova FJ. The radiobiology of radiosurgery and stereotactic radiotherapy. *Medical Dosimetry*. 1998;23(3):201-7.
36. Regaud T, Nogier T. Sterilization roentgenienne totale et definitive sans radiodermite, des testicules du belier adulte. Conditions de sa realisation. *Compt Rend Soc*. 1911;70:202-3.
37. Isaacson SR, Close LG. Chapter 11. Clinical Radiation Biology and Radiotherapy. In: Van-De-Water TR, Staecker H, editors. *Otolaryngology Basic Science and Clinical Review* New York: Thieme; 2005. p. 158-63.
38. Elkind MM, Sutton H. Radiation response of mammalian cells grown in culture. 1. Repair of X-ray damage in surviving Chinese hamster cells. *Radiation Research*. 1960;13:556-93.
39. Moulder JE, Rockwell S. Hypoxic fractions of solid tumors: experimental techniques, methods of analysis, and a survey of existing data. *International Journal of Radiation Oncology, Biology, Physics*. 1984;10(5):695-712.

40. Puck TT, Marcus PI. Action of x-rays on mammalian cells. *The Journal of experimental medicine*. 1956;103(5):653-66.
41. Altas E, Ertekin MV, Kuduban O, Gundogdu C, Demirci E, Sutbeyaz Y. Effects of piracetam supplementation on cochlear damage occurring in guinea pigs exposed to irradiation. *Biological and Pharmaceutical Bulletin*. 2006;29(7):1460-5.
42. Emami B, Lyman J, Brown A, Coia L, Goitein M, Munzenrider JE, et al. Tolerance of Normal Tissue to Therapeutic Irradiation. *International Journal of Radiation Oncology Biology Physics*. 1991;21(1):109-22.
43. Kwong DL, Wei WI, Sham JS, Ho WK, Yuen PW, Chua DT, et al. Sensorineural hearing loss in patients treated for nasopharyngeal carcinoma: a prospective study of the effect of radiation and cisplatin treatment. *International Journal of Radiation Oncology, Biology, Physics*. 1996;36(2):281-9.
44. Stieber VW, Mehta MP. Advances in radiation therapy for brain tumors. *Neurologic Clinics*. 2007;25(4):1005-33, ix.
45. Hussey DH, Wen BC. The Temporal Bone, Ear, and Paraganglia. In: Cox JD, Ang KK, editors. *Radiation Oncology Rationale Techniques Results*: Mosby Elsevier; 2010. p. 321-30.
46. Stell PM. Carcinoma of the external auditory meatus and middle ear. *Clinical otolaryngology and allied sciences*. 1984;9(5):281-99.
47. O'Neill JV, Katz AH, Skolnik EM. Otolologic complications of radiation therapy. *Otolaryngol Head Neck Surg* (1979). 1979;87(3):359-63. Epub 1979/05/01.
48. Brill AH, Martin MM, Fitz-Hugh GS, Constable WC. Postoperative and postradiotherapeutic serous otitis media. *Archives of Otolaryngology-Head & Neck Surgery*. 1974;99(6):406-8.
49. Borsanyi SJ, Blanchard CL. Ionizing radiation and the ear. *JAMA*. 1962;181:958-61.
50. Kveton JF, Sotelo-Avila C. Osteoradionecrosis of the ossicular chain. *American Journal of Otology*. 1986;7(6):446-8.
51. Pan CC, Eisbruch A, Lee JS, Snorrason RM, Ten Haken RK, Kileny PR. Prospective study of inner ear radiation dose and hearing loss in head-and-neck cancer patients. *International Journal of Radiation Oncology, Biology, Physics*. 2005;61(5):1393-402.
52. Honore HB, Bentzen SM, Moller K, Grau C. Sensori-neural hearing loss after radiotherapy for nasopharyngeal carcinoma: individualized risk estimation. *Radiotherapy and Oncology*. 2002;65(1):9-16.
53. Probst R, Grevers G, Iro H. *Basic Otolaryngology: A Step-by-Step Learning Guide*.: Thieme; 2005 November.

54. Roush J, Grose J. Chapter 30. Principles of Audiometry. In: Van-De-Water TR, Staecker H, editors. *Otolaryngology Basic Science and Clinical Review*. New-York: Thieme 2005. p. 374-84.
55. A. G. Shoup, Roeser RJ. Chapter 15. Audiologic Evaluation of Special Populations. In: Roeser R, Valente M, Hosford-Dunn H, editors. *Audiology Diagnosis*. 2nd edition ed. New-York: Thieme; 2007. p. 314-33.
56. Hofstetter P, Ding D, Powers N, Salvi RJ. Quantitative relationship of carboplatin dose to magnitude of inner and outer hair cell loss and the reduction in distortion product otoacoustic emission amplitude in chinchillas. *Hearing Research*. 1997;112(1-2):199-215.
57. Arnold A. Chapter 20. The Auditory Brainstem Response. In: Roeser R, Valente M, Hosford-Dunn H, editors. *Audiology Diagnosis*. New York: Thieme; 2007. p. 426-44.
58. Hall JW. *New Handbook of Auditory Evoked Responses*. Boston: Pearson Education; 2007.
59. Moller AR. Physiology of the auditory pathways with special reference to the auditory brain stem response (ABR). In: Pinheiro ML, Musiek FE, editors. *Assessment of central auditory dysfunction Foundations and clinical correlates*. Baltimore: Williams & Wilkins 1985. p. 23-41.
60. Wada SI, Starr A. Generation of auditory brain stem responses (ABRs). III. Effects of lesions of the superior olive, lateral lemniscus and inferior colliculus on the ABR in guinea pig. *Electroencephalography and Clinical Neurophysiology*. 1983;56(4):352-66.
61. Durrant JD, Martin WH, Hirsch B, Schwegler J. 3CLT ABR analyses in a human subject with unilateral extirpation of the inferior colliculus. *Hearing Research*. 1994;72(1-2):99-107.
62. Purdy SC, Houghton JM, Keith WJ, Greville KA. Frequency-specific auditory brainstem responses. Effective masking levels and relationship to behavioural thresholds in normal hearing adults. *Audiology*. 1989;28(2):82-91.
63. Stapells DR. Threshold estimation by the tone-evoked auditory brainstem response: a literature meta-analysis. *Journal of Speech-Language Pathology & Audiology*. 2000;24:74-83.
64. Grau C, Moller K, Overgaard M, Overgaard J, Elbrond O. Sensori-neural hearing loss in patients treated with irradiation for nasopharyngeal carcinoma. *International Journal of Radiation Oncology, Biology, Physics*. 1991;21(3):723-8.
65. Bhandare N, Antonelli PJ, Morris CG, Malayapa RS, Mendenhall WM. Ototoxicity after radiotherapy for head and neck tumors. *International Journal of Radiation Oncology, Biology, Physics*. 2007;67(2):469-79.

66. Downs SH, Black N. The feasibility of creating a checklist for the assessment of the methodological quality both of randomised and non-randomised studies of health care interventions. *Journal of Epidemiology and Community Health*. 1998;52(6):377-84.
67. Li JJ, Guo YK, Tang QL, Li SS, Zhang XL, Wu PA, et al. Prospective study of sensorineural hearing loss following radiotherapy for nasopharyngeal carcinoma. *Journal of Laryngology & Otology*. 2010;124(1):32-6.
68. Sumitsawan Y, Chaiyasate S, Chitapanarux I, Anansuthiwara M, Roongrotwattanasiri K, Vaseenon V, et al. Late complications of radiotherapy for nasopharyngeal carcinoma. *Auris, Nasus, Larynx*. 2009;36(2):205-9.
69. Yilmaz YF, Aytas FI, Akdogan O, Sari K, Savas ZG, Titiz A, et al. Sensorineural hearing loss after radiotherapy for head and neck tumors: a prospective study of the effect of radiation. *Otology and Neurotology*. 2008;29(4):461-3.
70. Low WK, Burgess R, Fong KW, Wang DY. Effect of radiotherapy on retro-cochlear auditory pathways. *Laryngoscope*. 2005;115(10):1823-6.
71. Wang LF, Kuo WR, Ho KY, Lee KW, Lin CS. A long-term study on hearing status in patients with nasopharyngeal carcinoma after radiotherapy. *Otology and Neurotology*. 2004;25(2):168-73.
72. Leighton SE, Kay R, Leung SF, Woo JK, Van Hasselt CA. Auditory brainstem responses after radiotherapy for nasopharyngeal carcinoma. *Clinical otolaryngology and allied sciences*. 1997;22(4):350-4.
73. Wakisaka H, Yamada H, Motoyoshi K, Ugumori T, Takahashi H, Hyodo M. Incidence of long-term ipsilateral and contralateral ototoxicity following radiotherapy for nasopharyngeal carcinoma. *Auris, Nasus, Larynx*. 2011;38(1):95-100.
74. Chan SH, Ng WT, Kam KL, Lee MC, Choi CW, Yau TK, et al. Sensorineural hearing loss after treatment of nasopharyngeal carcinoma: a longitudinal analysis. *International Journal of Radiation Oncology, Biology, Physics*. 2009;73(5):1335-42.
75. Chen WC, Liao CT, Tsai HC, Yeh JY, Wang CC, Tang SG, et al. Radiation-induced hearing impairment in patients treated for malignant parotid tumor. *Annals of Otology, Rhinology and Laryngology*. 1999;108(12):1159-64.
76. Schot LJ, Hilgers FJ, Keus RB, Schouwenburg PF, Dreschler WA. Late effects of radiotherapy on hearing. *European Archives of Oto-Rhino-Laryngology*. 1992;249(6):305-8.
77. Munro AJ. An overview of randomised controlled trials of adjuvant chemotherapy in head and neck cancer. *British Journal of Cancer*. 1995;71(1):83-91.

78. Vokes EE. Induction chemotherapy for head and neck cancer: recent data. *Oncologist*. 2010;15 Suppl 3:3-7.
79. Rybak LP, Whitworth CA, Mukherjea D, Ramkumar V. Mechanisms of cisplatin-induced ototoxicity and prevention. *Hearing Research*. 2007;226(1-2):157-67.
80. Cox JD, Stetz J, Pajak TF. Toxicity criteria of the Radiation Therapy Oncology Group (RTOG) and the European Organization for Research and Treatment of Cancer (EORTC). *International Journal of Radiation Oncology, Biology, Physics*. 1995;31(5):1341-6.
81. Pavy JJ, Denekamp J, Letschert J, Littbrand B, Mornex F, Bernier J, et al. EORTC Late Effects Working Group. Late effects toxicity scoring: the SOMA scale. *Radiotherapy and Oncology*. 1995;35(1):11-5.
82. Bhide SA, Harrington KJ, Nutting CM. Otological toxicity after postoperative radiotherapy for parotid tumours. *Clinical Oncology (Royal College of Radiologists)*. 2007;19(1):77-82.
83. Bhandare N, Jackson A, Eisbruch A, Pan CC, Flickinger JC, Antonelli P, et al. Radiation therapy and hearing loss. *International Journal of Radiation Oncology, Biology, Physics*. 2010;76(3 Suppl):S50-7.
84. Grewal S, Merchant T, Reymond R, McInerney M, Hodge C, Shearer P. Auditory late effects of childhood cancer therapy: a report from the Children's Oncology Group. *Pediatrics*. 2010;125(4):e938-50.
85. Parham K, McKinnon BJ, Eibling D, Gates GA. Challenges and opportunities in presbycusis. *Otolaryngology-head and neck surgery*. 2011;144(4):491-5.
86. Grau C, Moller K, Overgaard M, Overgaard J, Elbrond O. Auditory brain stem responses in patients after radiation therapy for nasopharyngeal carcinoma. *Cancer*. 1992;70(10):2396-401.
87. Verheij M, Bartelink H. Radiation-induced apoptosis. *Cell and Tissue Research*. 2000;301(1):133-42.
88. Shinomiya N. New concepts in radiation-induced apoptosis: 'premitotic apoptosis' and 'postmitotic apoptosis'. *Journal of Cellular and Molecular Medicine*. 2001;5(3):240-53.
89. Low WK, Tan MG, Sun L, Chua AW, Goh LK, Wang DY. Dose-dependant radiation-induced apoptosis in a cochlear cell-line. *Apoptosis*. 2006;11(12):2127-36.
90. Chao C, Saito S, Anderson CW, Appella E, Xu Y. Phosphorylation of murine p53 at ser-18 regulates the p53 responses to DNA damage. *Proceedings of the National Academy of Sciences of the United States of America*. 2000;97(22):11936-41.

91. Bentzen SM. Preventing or reducing late side effects of radiation therapy: radiobiology meets molecular pathology. *Nature Reviews Cancer*. 2006;6(9):702-13.
92. Azzam EI, Jay-Gerin JP, Pain D. Ionizing radiation-induced metabolic oxidative stress and prolonged cell injury. *Cancer Letters*. 2011.
93. Zhao W, Diz DI, Robbins ME. Oxidative damage pathways in relation to normal tissue injury. *British Journal of Radiology*. 2007;80 Spec No 1:S23-31.
94. Mikkelsen RB, Wardman P. Biological chemistry of reactive oxygen and nitrogen and radiation-induced signal transduction mechanisms. *Oncogene*. 2003;22(37):5734-54.
95. Cadenas E, Davies KJ. Mitochondrial free radical generation, oxidative stress, and aging. *Free Radical Biology and Medicine*. 2000;29(3-4):222-30.
96. Leach JK, Black SM, Schmidt-Ullrich RK, Mikkelsen RB. Activation of constitutive nitric-oxide synthase activity is an early signaling event induced by ionizing radiation. *Journal of Biological Chemistry*. 2002;277(18):15400-6.
97. Richter C, Park JW, Ames BN. Normal oxidative damage to mitochondrial and nuclear DNA is extensive. *Proceedings of the National Academy of Sciences of the United States of America*. 1988;85(17):6465-7.
98. Yakes FM, Van Houten B. Mitochondrial DNA damage is more extensive and persists longer than nuclear DNA damage in human cells following oxidative stress. *Proceedings of the National Academy of Sciences of the United States of America*. 1997;94(2):514-9.
99. Ye K, Ji CB, Lu XW, Ni YH, Gao CL, Chen XH, et al. Resveratrol attenuates radiation damage in *Caenorhabditis elegans* by preventing oxidative stress. *Journal of radiation research*. 2010;51(4):473-9.
100. Rybak LP, Whitworth CA. Ototoxicity: therapeutic opportunities. *Drug Discovery Today*. 2005;10(19):1313-21.
101. Le Prell CG, Yamashita D, Minami SB, Yamasoba T, Miller JM. Mechanisms of noise-induced hearing loss indicate multiple methods of prevention. *Hearing Research*. 2007;226(1-2):22-43.
102. Sha SH, Taylor R, Forge A, Schacht J. Differential vulnerability of basal and apical hair cells is based on intrinsic susceptibility to free radicals. *Hearing Research*. 2001;155(1-2):1-8.
103. Usami S, Hjelle OP, Ottersen OP. Differential cellular distribution of glutathione--an endogenous antioxidant--in the guinea pig inner ear. *Brain Research*. 1996;743(1-2):337-40.
104. Novotny O. [Effect of x-rays on cochlea of guinea pig]. *Archivio Italiano di Otologia, Rinologia e Laringologia*. 1951;62(1):15-9. Sull'azione dei raggi x sulla chiocciola della cavia.

105. Kozlov M. Changes in the peripheric section of the auditory analyzer in acute radiation sickness. *ORL J Otorhinolaryngol Relat Spec.* 1959;21:29-35.
106. Hoistad DL, Ondrey FG, Mutlu C, Schachern PA, Paparella MM, Adams GL. Histopathology of human temporal bone after cis-platinum, radiation, or both. *Otolaryngology - Head and Neck Surgery.* 1998;118(6):825-32.
107. Winther FO. X-ray irradiation of the inner ear of the guinea pig. Early degenerative changes in the cochlea. *Acta Oto-Laryngologica.* 1969;68(1):98-117.
108. Kim CS, Shin SO. Ultrastructural changes in the cochlea of the guinea pig after fast neutron irradiation. *Otolaryngology - Head and Neck Surgery.* 1994;110(4):419-27.
109. Tokimoto T, Kanagawa K. Effects of X-ray irradiation on hearing in guinea pigs. *Acta Oto-Laryngologica.* 1985;100(3-4):266-72.
110. Bohne BA, Marks JE, Glasgow GP. Delayed effects of ionizing radiation on the ear. *The Laryngoscope.* 1985;95(7 Pt 1):818-28.
111. Rubin P. The Franz Buschke lecture: late effects of chemotherapy and radiation therapy: a new hypothesis. *International Journal of Radiation Oncology, Biology, Physics.* 1984;10(1):5-34.
112. Patt HM, Tyree EB, Straube RL, Smith DE. Cysteine Protection against X Irradiation. *Science.* 1949;110(2852):213-4.
113. Brizel DM, Wasserman TH, Henke M, Strnad V, Rudat V, Monnier A, et al. Phase III randomized trial of amifostine as a radioprotector in head and neck cancer. *Journal of Clinical Oncology.* 2000;18(19):3339-45.
114. Yuhas J, Spellman J, Culo F. The role of WR2721 in radiotherapy and-or chemotherapy. In: K B, editor. *Radiation sensitizers.* New York: Masson Publishing; 1980.
115. Low WK, Sun L, Tan MG, Chua AW, Wang DY. L-N-Acetylcysteine protects against radiation-induced apoptosis in a cochlear cell line. *Acta otolaryngologica.* 2008;128(4):440-5.
116. Lessa RM, Oliveira JA, Rossato M, Ghilardi Netto T. Analysis of the cytoprotective effect of amifostine on the irradiated inner ear of guinea pigs: an experimental study. *Brazilian journal of Otorhinolaryngology.* 2009;75(5):694-700.
117. Yang X, Lu Y, Xie D. [Protective effect of Radix Salvia Miltiorrhizae on radiation damage of the cochlea]. *Hunan Yi Ke Da Xue Xue Bao (Bulletin of Hunan Medical University).* 1999;24(5):465-7.
118. Altas E, Ertekin MV, Gundogdu C, Demirci E. L-carnitine reduces cochlear damage induced by gamma irradiation in Guinea pigs. *Annals of Clinical and Laboratory Science.* 2006;36(3):312-8.

119. Pyun JH, Kang SU, Hwang HS, Oh YT, Kang SH, Lim YA, et al. Epicatechin inhibits radiation-induced auditory cell death by suppression of reactive oxygen species generation. *Neuroscience*. 2011;199:410-20.
120. Chakraborty A, Chowdhury S, Bhattacharyya M. Effect of Metformin on oxidative stress, nitrosative stress and inflammatory biomarkers in type 2 diabetes patients. *Diabetes Research and Clinical Practice*. 2011;93(1):56-62.
121. Jalving M, Gietema JA, Lefrandt JD, de Jong S, Reyners AK, Gans RO, et al. Metformin: taking away the candy for cancer? *European Journal of Cancer*. 2010;46(13):2369-80.
122. Tucker GT, Casey C, Phillips PJ, Connor H, Ward JD, Woods HF. Metformin kinetics in healthy subjects and in patients with diabetes mellitus. *British Journal of Clinical Pharmacology*. 1981;12(2):235-46. Epub 1981/08/01.
123. Wilcock C, Bailey CJ. Accumulation of Metformin by tissues of the normal and diabetic mouse. *Xenobiotica*. 1994;24(1):49-57.
124. Wilcock C, Wyre ND, Bailey CJ. Subcellular distribution of Metformin in rat liver. *Journal of Pharmacy and Pharmacology*. 1991;43(6):442-4.
125. Labuzek K, Suchy D, Gabryel B, Bielecka A, Liber S, Okopien B. Quantification of Metformin by the HPLC method in brain regions, cerebrospinal fluid and plasma of rats treated with lipopolysaccharide. *Pharmacological Reports*. 2010;62(5):956-65.
126. Lv WS, Wen JP, Li L, Sun RX, Wang J, Xian YX, et al. The effect of Metformin on food intake and its potential role in hypothalamic regulation in obese diabetic rats. *Brain Research*. 2012;1444:11-9.
127. Kimura N, Masuda S, Tanihara Y, Ueo H, Okuda M, Katsura T, et al. Metformin is a superior substrate for renal organic cation transporter OCT2 rather than hepatic OCT1. *Drug Metabolism and Pharmacokinetics*. 2005;20(5):379-86.
128. Ciarimboli G, Deuster D, Knief A, Sperling M, Holtkamp M, Edemir B, et al. Organic cation transporter 2 mediates cisplatin-induced oto- and nephrotoxicity and is a target for protective interventions. *American Journal of Pathology*. 2010;176(3):1169-80.
129. Bonnefont-Rousselot D, Raji B, Walrand S, Gardes-Albert M, Jore D, Legrand A, et al. An intracellular modulation of free radical production could contribute to the beneficial effects of Metformin towards oxidative stress. *Metabolism: Clinical and Experimental*. 2003;52(5):586-9.
130. Khouri H, Collin F, Bonnefont-Rousselot D, Legrand A, Jore D, Gardes-Albert M. Radical-induced oxidation of Metformin. *European Journal of Biochemistry*. 2004;271(23-24):4745-52.

131. Algire C, Moiseeva O, Deschenes-Simard X, Amrein L, Petruccelli L, Birman E, et al. Metformin reduces endogenous reactive oxygen species and associated DNA damage. *Cancer prevention research (Philadelphia, Pa)*. 2012;5(4):536-43.
132. Libby G, Donnelly LA, Donnan PT, Alessi DR, Morris AD, Evans JM. New users of Metformin are at low risk of incident cancer: a cohort study among people with type 2 diabetes. *Diabetes Care*. 2009;32(9):1620-5.
133. Jiralerspong S, Palla SL, Giordano SH, Meric-Bernstam F, Liedtke C, Barnett CM, et al. Metformin and pathologic complete responses to neoadjuvant chemotherapy in diabetic patients with breast cancer. *Journal of Clinical Oncology*. 2009;27(20):3297-302.
134. Anisimov VN, Berstein LM, Egormin PA, Piskunova TS, Popovich IG, Zabezhinski MA, et al. Effect of Metformin on life span and on the development of spontaneous mammary tumors in HER-2/neu transgenic mice. *Experimental Gerontology*. 2005;40(8-9):685-93.
135. Tomimoto A, Endo H, Sugiyama M, Fujisawa T, Hosono K, Takahashi H, et al. Metformin suppresses intestinal polyp growth in ApcMin/+ mice. *Cancer Science*. 2008;99(11):2136-41.
136. Algire C, Zakikhani M, Blouin MJ, Shuai JH, Pollak M. Metformin attenuates the stimulatory effect of a high-energy diet on in vivo LLC1 carcinoma growth. *Endocrine-Related Cancer*. 2008;15(3):833-9.
137. Thoreen CC, Sabatini DM. AMPK and p53 help cells through lean times. *Cell Metabolism*. 2005;1(5):287-8.
138. Buzzai M, Jones RG, Amaravadi RK, Lum JJ, DeBerardinis RJ, Zhao F, et al. Systemic treatment with the antidiabetic drug Metformin selectively impairs p53-deficient tumor cell growth. *Cancer Research*. 2007;67(14):6745-52.
139. Zannella VE, Cojocari D, Hilgendorf S, Vellanki RN, Chung S, Wouters BG, et al. AMPK regulates metabolism and survival in response to ionizing radiation. *Radiotherapy and oncology : journal of the European Society for Therapeutic Radiology and Oncology*. 2011;99(3):293-9. Epub 2011/07/01.
140. Sanli T, Rashid A, Liu C, Harding S, Bristow RG, Cutz JC, et al. Ionizing radiation activates AMP-activated kinase (AMPK): a target for radiosensitization of human cancer cells. *International Journal of Radiation Oncology, Biology, Physics*. 2010;78(1):221-9.
141. Kalinec F, Kalinec G, Boukhvalova M, Kachar B. Establishment and characterization of conditionally immortalized organ of corti cell lines. *Cell Biology International*. 1999;23(3):175-84.
142. Kalinec GM, Webster P, Lim DJ, Kalinec F. A cochlear cell line as an in vitro system for drug ototoxicity screening. *Audiology and Neuro-Otology*. 2003;8(4):177-89.

143. Cory AH, Owen TC, Barltrop JA, Cory JG. Use of an aqueous soluble tetrazolium/formazan assay for cell growth assays in culture. *Cancer Communications*. 1991;3(7):207-12. Epub 1991/07/01.
144. Verhaegen F, Granton P, Tryggestad E. Small animal radiotherapy research platforms. *Physics in Medicine and Biology*. 2011;56(12):R55-83.
145. Greene JS, Giddings NA, Jacobson JT. Effect of irradiation on guinea pig ABR thresholds. *Otolaryngology - Head and Neck Surgery*. 1992;107(6 Pt 1):763-8.
146. ISP. Gafchromic EBT. Self-developing film for radiotherapy dosimetry. *Advanced Materials*. USA: International Specialty Products; 2007.
147. McLaughlin WL, Miller A, Fidan S, Pejtersen K, Batsberg Pedersen W. Radiochromic plastic films for accurate measurement of radiation absorbed dose and dose distributions. *Radiation Physics and Chemistry* (1977). 1977;10(2):119-27.
148. Chiu-Tsao ST, Ho Y, Shankar R, Wang L, Harrison LB. Energy dependence of response of new high sensitivity radiochromic films for megavoltage and kilovoltage radiation energies. *Medical Physics*. 2005;32(11):3350-4.
149. Butson MJ, Yu PKN, Cheung T, Metcalfe P. Radiochromic film for medical radiation dosimetry. *Materials Science & Engineering R-Reports*. 2003;41(3-5):61-120.
150. White DR. Tissue substitutes in experimental radiation physics. *Medical Physics*. 1978;5(6):467-79.
151. Kirby BJ, Davis JR, Grant JA, Morgan MJ. Extracting material parameters from x-ray attenuation: a CT feasibility study using kilovoltage synchrotron x-rays incident upon low atomic number absorbers. *Physics in Medicine and Biology*. 2003;48(20):3389-409.
152. Niroomand-Rad A, Blackwell CR, Coursey BM, Gall KP, Galvin JM, McLaughlin WL, et al. Radiochromic film dosimetry: Recommendations of AAPM Radiation Therapy Committee Task Group 55. *Medical Physics*. 1998;25(11):2093-115.
153. Devic S, Seuntjens J, Sham E, Podgorsak EB, Schmidtlein CR, Kirov AS, et al. Precise radiochromic film dosimetry using a flat-bed document scanner. *Medical Physics*. 2005;32(7):2245-53.
154. Ma CM, Coffey CW, DeWerd LA, Liu C, Nath R, Seltzer SM, et al. AAPM protocol for 40-300 kV x-ray beam dosimetry in radiotherapy and radiobiology. *Medical Physics*. 2001;28(6):868-93.
155. Gamble JE, Peterson EA, Chandler JR. Radiation effects on the inner ear. *Archives of Otolaryngology-Head & Neck Surgery*. 1968;88(2):156-61.
156. Nagel D, Schafer J. Changes in cochlear microphonic response after Y-ray irradiation of the inner ear of the guinea-pig. *Archives of Oto-Rhino-Laryngology*. 1984;241(1):17-21.

157. Miller MW, Riedel G, Hoistad D, Sutherland C, Juhn SK, Adams GL, et al. Ototoxicity after combined platinum and fractionated radiation in a novel guinea pig model. *American Journal of Otolaryngology*. 2009;30(1):1-7.
158. Ohashi Y, Nakai Y, Esaki Y, Ikeoka H, Koshimo H, Onoyama Y. Acute effects of irradiation on middle ear mucosa. *Annals of Otolaryngology, Rhinology and Laryngology*. 1988;97(2 Pt 1):173-8.
159. Johannesen TB, Rasmussen K, Winther FO, Halvorsen U, Lote K. Late radiation effects on hearing, vestibular function, and taste in brain tumor patients. *International Journal of Radiation Oncology Biology Physics*. 2002;53(1):86-90.
160. Olfert ED CB, McWilliam AA, editor. *Guide to the care and use of experimental animals*. 2nd ed. Ottawa: Canadian Council on Animal Care; 1993.
161. Kuhnle HF, Wolff HP, Schmidt FH, Reiter R. Blood-glucose-lowering activity of 2-(3-phenylpropoxyimido)-butyrate (BM 13.677). *Biochemical Pharmacology*. 1990;40(8):1821-5.
162. Bulterijs S. Metformin as a geroprotector. *Rejuvenation Research*. 2011;14(5):469-82.